Structural Biology and Molecular Biophysics
Physics of Living Systems

Single-molecule imaging reveals the roles of the membrane-binding motif and the C-terminal domain of RNase E in its localization and diffusion in *Escherichia coli*

Reviewed Preprint
v2 • October 24, 2025
Revised by authors

Reviewed Preprint
v1 • January 29, 2025

Laura Troyer, Yu-Huan Wang, Shobhna Shobhna, Seunghyeon Kim, Brooke Ramsey, Jeechul Woo, Emad Tajkhorshid, Sangjin Kim

Department of Physics, University of Illinois Urbana-Champaign, Urbana, United States • Theoretical and Computational Biophysics Group, NIH Center for Macromolecular Modeling and Visualization, Beckman Institute for Advanced Science and Technology, University of Illinois Urbana-Champaign, Urbana, United States • Department of Biochemistry, University of Illinois Urbana-Champaign, Urbana, United States • Center for Biophysics and Quantitative Biology, University of Illinois Urbana–Champaign, Urbana, United States • Moduli Technologies, LLC, Springfield, United States

eLife Assessment

This **valuable** study uses single-molecule imaging to characterize factors controlling the localization, mobility, and function of RNase E in E. coli, a key bacterial ribonuclease central to mRNA catabolism. The supporting evidence for the differential roles of RNAse E's membrane targeting sequence (MTS) and the C-terminal domain (CTD) to RNAse E's diffusion and membrane association is **convincing**. It provides insight into how RNAse E shapes the spatiotemporal organization of RNA processing in bacterial cells. This interdisciplinary work will be of interest to cell biologists, microbiologists, biochemists, and biophysicists.

https://doi.org/10.7554/eLife.105062.2.sa4

Abstract

In *Escherichia coli*, RNase E, a central enzyme in RNA processing and mRNA degradation, contains a catalytic N-terminal domain (NTD), a membrane-targeting sequence (MTS), and a C-terminal domain (CTD). We investigated how MTS and CTD influence RNase E localization, diffusion, and function. Super-resolution microscopy revealed that ~93% of RNase E localizes to the inner membrane and exhibits slow diffusion similar to polysomes. Comparing the native amphipathic MTS with a transmembrane motif showed that the MTS confers slower diffusion and stronger membrane binding. The CTD further slows diffusion by increasing mass but unexpectedly weakens membrane association. RNase E mutants with partial cytoplasmic localization displayed enhanced co-transcriptional degradation of *lacZ* mRNA.

These findings indicate that variations in the MTS and the presence of the CTD shape the spatiotemporal organization of RNA processing in bacterial cells, providing mechanistic insight into how RNase E domain architecture influences its cellular function.

Introduction

RNase E (RNE) is the main endoribonuclease in *Escherichia coli*, known for its role in RNA processing and mRNA degradation[1–3]. It is an essential protein[4,5], and homologous proteins are found across many bacterial species[6–8]. The essentiality stems from the N-terminal domain (NTD), or the catalytic domain[9]. The NTD is followed by a membrane targeting sequence (MTS) and the C-terminal domain (CTD), or macromolecular interaction domain[2], where RhlB (a DEAD-box RNA helicase), PNPase (a 3'→5' exonuclease), and enolase (a glycolytic enzyme) bind to form the RNA degradosome complex[6]. The MTS forms an amphipathic α helix, responsible for the localization of RNE on the inner membrane[10,11]. Interestingly, the membrane localization of RNE and the presence of the CTD are not essential in *E. coli* nor are they conserved across bacterial species, in contrast to the broad conservation of the NTD across bacteria as well as chloroplasts[7,12,13]. This raises a question about the roles of membrane localization and the CTD in the *in vivo* function of RNE.

E. coli strains with cytoplasmic RNE (due to the removal of the MTS) are viable, although they grow more slowly than the wild-type (WT) cells[10,14]. *In vitro* studies have shown that membrane binding of RNE does not necessarily increase its enzymatic activity[10,14]. However, membrane localization is likely important for gene regulation *in vivo* because RNE becomes sequestered from the cytoplasmic pool of mRNAs, giving mRNAs time for translation. This idea is supported by our recent observation that the membrane-bound RNE limits the degradation of nascent mRNAs while cytoplasmic RNE (ΔMTS) can degrade nascent mRNAs during transcription[15]. We found that transcripts encoding membrane proteins can be an exception to this rule, in that they can experience co-transcriptional degradation assisted by the transertion effect[15]. These findings agree with results from a genome-wide study, indicating that the membrane localization of RNE allows for differential regulation of mRNA stability for genes encoding cytoplasmic proteins versus inner membrane proteins in *E. coli*[16].

Previous studies have reported evidence that *E. coli* RNE can localize in the cytoplasm—for example, when cells were grown anaerobically[17] or when membrane fluidity was reduced by changes in lipid composition[18]. These findings imply that RNE can dissociate from the membrane; however, the origin of its weak membrane binding remains unknown.

Across bacteria, several species within α-proteobacteria have cytoplasmic RNE[19] while other species possess membrane-bound RNE. Among these, *B. subtilis* RNase Y (a functional homolog of RNE) associates with the membrane via a transmembrane (TM) motif[20], instead of an amphipathic motif used by *E. coli* and other γ-proteobacteria[7]. Given the diversity of membrane-binding motifs that have arisen through evolution, it should be possible to engineer *E. coli* RNE with a TM motif. Such a mutant would provide a useful model for investigating the impact of membrane-binding motifs on the localization, diffusion, and activity of RNE.

Lastly, the CTD of *E. coli* RNE is an intrinsically disordered region[21] that, while nonessential for cell viability, enhances the enzymatic activity of the NTD[15,22–24]. As the primary binding site for degradosome components[6], the CTD is thought to facilitate mRNA degradation by recruiting these proteins near the catalytic NTD. However, our recent study showed that these associated proteins have minimal impact on the degradation rate of *lacZ* mRNA, whereas deletion of the CTD markedly stabilizes the transcript[15], suggesting a possible intramolecular allosteric effect within RNE. In the present study, we further show that the CTD modulates the membrane binding affinity of RNE, possibly by affecting its conformation. These results reveal a previously underappreciated

role of the CTD in regulating RNE function beyond degradosome assembly, with implications for how the spatial organization and structural dynamics of RNE fine-tune RNA degradation in bacteria.

In this study, we quantified the membrane binding percentage (MB%) of RNE in *E. coli* using single-molecule microscopy and showed that membrane association governs its diffusion and mRNA-degradation activity. Perturbing the native MTS, substituting it with LacY TM segments, and deleting the CTD collectively revealed how the MTS and CTD set RNE's spatial organization and provided routes for tuning activity through subcellular control.

Results

Membrane binding percentage (MB%) of RNE

First, we investigated the subcellular localization of RNE in live cells. Previous fluorescence microscopy studies have shown that RNE is localized to the inner membrane in *E. coli*[10,11,16], but the percentage of membrane-bound molecules has not been quantitatively examined in live cells. To address this gap, we fused RNE with a photo-convertible fluorescent protein, mEos3.2[25] and imaged individual RNE molecules over time in two dimensions (**Fig. 1A**). The positions of fluorescent molecules were identified in each frame and linked into trajectories using the open-source software u-track[26] (**Fig. 1A**). In this section, we analyze localization, and diffusion dynamics are addressed in subsequent sections.

Subcellular locations were calculated relative to the cell boundaries identified from bright-field images using another open-source image analysis package Oufti[27] (**Fig 1B**). To combine data from many cells, molecular positions along the short and long axes of a cell were normalized to the cell width and cell length, yielding xNorm and yNorm, respectively (**Fig. 1C**). Based on yNorm, molecules within the cylindrical part of the cell were selected, and their xNorm values were used to generate an xNorm histogram. Hereinafter, we focus on the xNorm histogram to compare the membrane enrichment across protein constructs.

The xNorm histogram of RNE shows two peaks corresponding to the inner membrane on each side of the cell (**Fig. 1D**, **Fig. S1A**), very similar to the xNorm histogram of LacY, obtained by imaging LacY-mEos3.2 using the same method. LacY is a membrane channel for lactose and is composed of 12 TM segments[28]. It is expected to be inserted into the inner membrane during translation[29–31], such that all imaged LacY is expected to be localized in the inner membrane[32].

We further quantified the percentage of molecules bound to the membrane (membrane-binding percentage or MB%) from the xNorm histogram. For this analysis, we first confirmed that proteins localized on the membrane and in the cytoplasm are detected with equal probability, despite differences in their mobilities (Fig. S1B-C). Next, we developed a mathematical model based on a 2D projection of molecules randomly distributed either on the surface of or within a cylinder. The model includes imaging effects that affect the shape of xNorm histograms: localization error, the limited focal depth of the quasi-TIRF illumination we used, and the location of the inner membrane relative to the cell boundary (Fig. S1D-G). Model fitting was performed using a Markov-Chain Monte Carlo algorithm (MCMC). For validation, we applied the model to xNorm histograms of LacY and LacZ, which serve as benchmarks for complete membrane binding and complete cytoplasmic localization, respectively. The MB% of LacY was 99% with a 95% confidence interval of [96%, 100%], and LacZ showed MB% of 3.4% [0.2%, 7.3%] (**Fig. 1E-F**). Both MB% agree with the expectations for membrane and cytoplasmic proteins. For RNE, we found an MB% of 93% [91%, 96%] (**Fig. 1E**). The xNorm histogram of the fastest 7% of the RNE population (based on

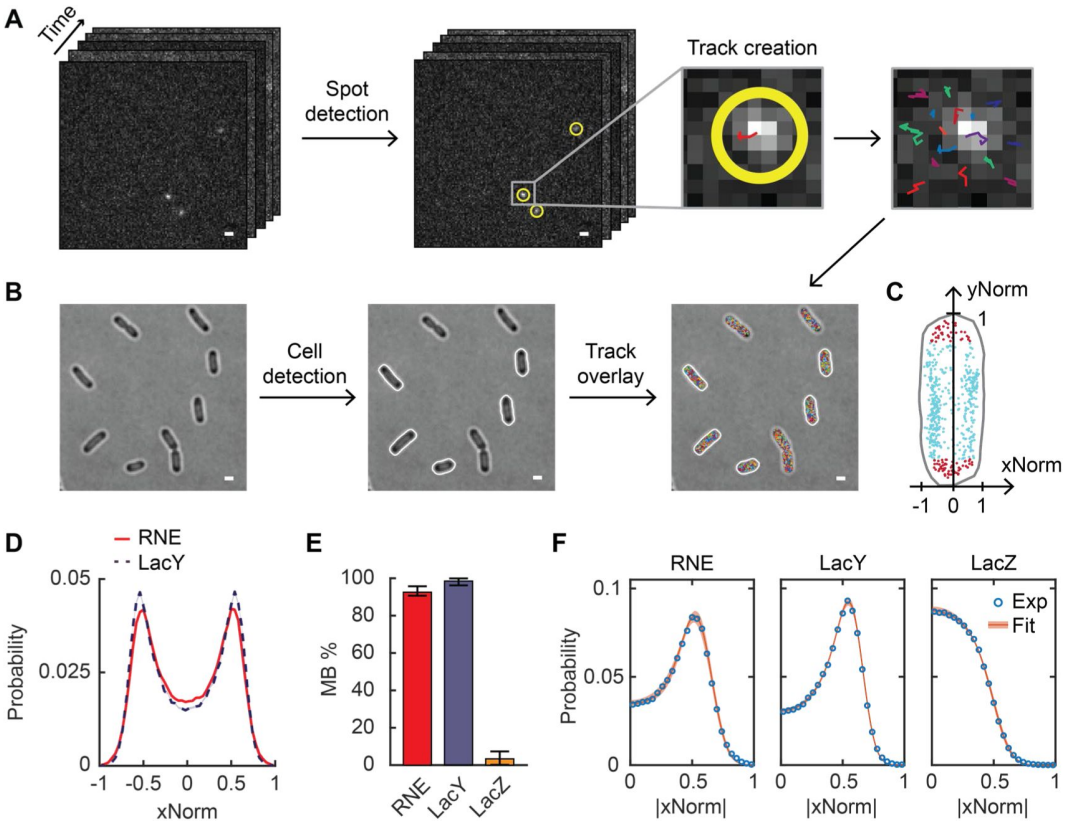

Figure 1

Analysis of single-molecule images for the subcellular localization and dynamics of proteins.

(**A**) Single-molecule image analysis. Spots were detected in each frame (highlighted with yellow circles), and tracks were created across frames (different colors were chosen for different tracks). (**B**) Cell detection. Cell outlines were determined from bright-field images. Only non-dividing cells were analyzed (indicated by white outlines). (**C**) Normalized position of spots of RNE along the short (x) and the long (y) axes of an example cell. Red spots are inside the cell endcaps, and cyan spots are in the cylindrical region of the cell. (**D**) xNorm histogram of RNE and LacY. Only spots in the cylindrical region of cells (like cyan spots in **C**) were included, totaling n = 143,000 spots. The standard error of the mean (SEM) calculated from bootstrapping is displayed as a shaded area but is smaller than the line width (see **Fig. S1A** for details). (**E**) The membrane binding percentage (MB%) of RNE, LacY, and LacZ. Error bars are from the 95% confidence interval. (**F**) Histogram of absolute xNorm and model fitting of RNE, LacY, and LacZ to determine MB%. Orange highlights indicate the range of xNorm expected based on the standard deviations in the parameter values estimated by MCMC. The white scale bars in panels **A-B** are 1 μm. See **Table S6** for data statistics.

the diffusion coefficient, as discussed below) exhibited a cytoplasmic localization pattern (without the two membrane-associated peaks), supporting the existence of a cytoplasmic RNE subpopulation (**Fig. S2A**).

We confirmed that the MTS (residue 568-582) is essential for the membrane binding of RNE, as deletion of the MTS sequence made the xNorm like that of LacZ (**Fig. 2A-B**, **Fig. S2D**). We note that the xNorm profile of RNE ΔMTS was slightly different from that of LacZ near the center line of the cell (x = 0), suggesting fewer RNE ΔMTS molecules were at the midline of the cell. Also, xNorm fitting yielded an MB% of 33%. These results may reflect nucleoid exclusion of RNE ΔMTS due to its large size[33]. Consistently, a smaller cytoplasmic RNE variant generated by CTD truncation (RNE (1-529) or RNE ΔMTS ΔCTD) exhibited a xNorm profile closer to that of LacZ (**Fig. 2B**, **Fig. S2E**).

Is there a critical residue(s) within the MTS required for membrane binding? The MTS forms an amphipathic α-helix, in which hydrophobic residues are expected to align on one side of the helix (**Fig. 2C**)[10]. Previous studies suggested that replacing one of the hydrophobic residues with a hydrophilic amino acid can disrupt membrane binding of RNE[10,11]. We revisited the point mutations discussed in Khemici et al[10] and analyzed MB% by mEos3.2 imaging. We found that the F574A F575A double mutation (noted as F574AA) did not significantly affect MB%, consistent with the fact that the substituted amino acids remain hydrophobic (**Fig. 2D-E**, **Fig. S2F**). In contrast, F582E and F575E mutations reduced MB% to 47% and 50%, respectively (**Fig. 2E**), and their xNorm histograms resembled that of RNE ΔMTS, suggesting predominantly cytoplasmic localization (**Fig. 2D**, **Fig. S2D**, **S2G-H**). These findings indicate that the phenylalanine residues at positions 575 and 582 are critical for membrane association of RNE.

Effect of membrane binding on the diffusion of RNE

The membrane localization of RNE likely limits its diffusion and interaction with mRNA targets. Additionally, interaction with ribosome-bound mRNAs can further slow the diffusion of RNE. Here, we examined how these factors contribute to the diffusion dynamics of RNE.

To measure the diffusion of RNE, we analyzed the trajectories of individual RNE-mEos3.2 imaged at a 21.7-ms acquisition interval (**Fig. 1A**). We calculated the diffusion coefficient D by fitting the mean-squared displacement (MSD) of each trajectory to the equation $MSD = 4D\tau + b$, where τ is lag time and b accounts for both dynamic and static localization errors[34] (**Fig. 3A**). We obtained $D_{RNE} = 0.0184 \pm 0.0002$ μm^2/s (mean ± SEM). This value was well above the lower detection limit of our microscope, determined using stationary, surface-immobilized mEos3.2, $D = 0.0020 \pm 0.0001$ μm^2/s (**Fig. S3A, Supplementary Discussion**). Notably, D_{RNE} was comparable to that of ribosome-bound mRNAs, estimated to be $D \sim 0.015$ μm^2/s based on the diffusion of ribosomal protein L1 (**Fig. S3B**).

To assess how membrane association affects diffusion, we compared D of WT RNE and the ΔMTS mutant. These two proteins have similar molecular masses, as the MTS comprises only 15 of the 1061 residues in a monomer of RNE (**Fig. 2A**). Therefore, any difference in D can be attributed to their subcellular localizations (membrane vs cytoplasm) rather than mass. We found that $D_{\Delta MTS}$ is ~5.5 times that of D_{RNE} (**Fig. 3B**).

We examined another pair of RNE mutants that differ in localization (membrane vs cytoplasm) but are similar in size: membrane-bound RNE (1-592) and cytoplasmic RNE (1-529), both lacking the CTD. These truncated variants diffused faster than their full-length counterparts due to reduced mass, but their D values still differed by a factor of ~5.3 due to localization (**Fig. 3B**). Together, these results suggest that the membrane binding reduces RNE mobility by a factor of 5.

Figure 2

Mutations in the MTS affecting the localization of RNE.

(**A**) Linear representation of the RNE monomer. The NTD and the CTD are defined as regions flanking the MTS. Numbers indicate the amino acid residues. (**B**) xNorm histograms of cytoplasmic RNE mutants. (**C**) Helical wheel diagram of the MTS region of RNE (residue 568-582). (**D**) xNorm histogram of RNE MTS point mutants. (**E**) MB% of RNE MTS point mutants. Error bars indicate the 95% confidence interval. In panels B and D, the SEM from bootstrapping is shown but is smaller than the line width. See **Table S6** for data statistics.

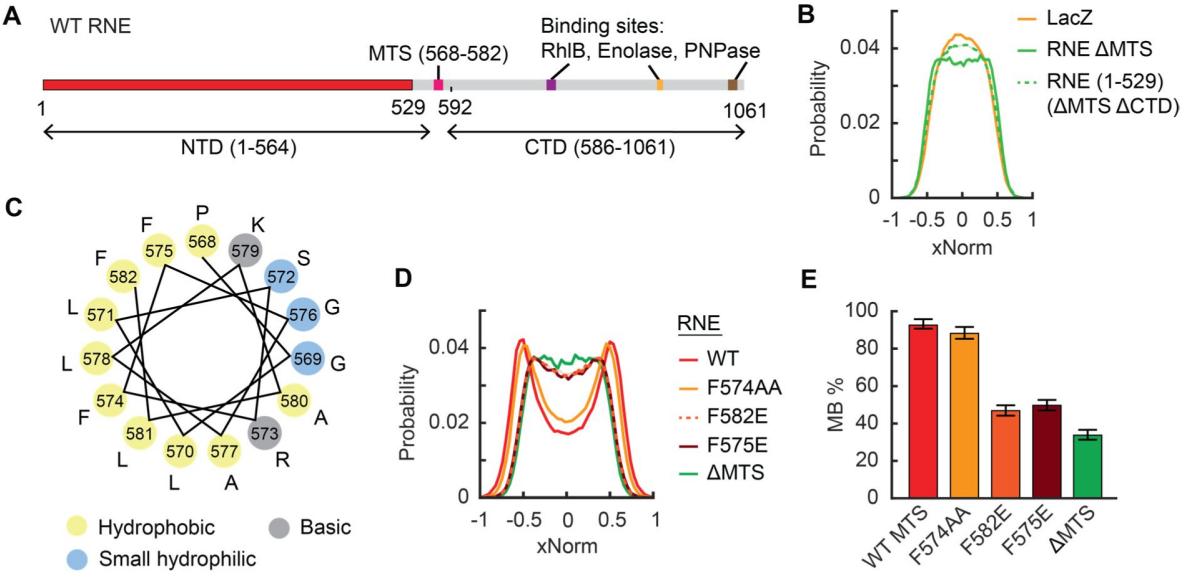

Figure 3

RNE diffusion, influenced by membrane binding and interactions with mRNAs.

(**A**) MSD versus time delay (τ) for RNE. Ensemble-averaged time-averaged (EATA) MSD was calculated by averaging the time-averaged MSD of individual tracks. (**B**) Mean diffusion coefficients of various RNE mutants, lacking the MTS and/or the CTD. (**C-E**) Change in the mean diffusion coefficient of RNE (**C**), LacY (**D**), and ribosome L1 protein (**E**) when cellular RNAs were depleted by rifampicin treatment. Error bars in panels B-E represent the SEM. See **Table S6** for data statistics.

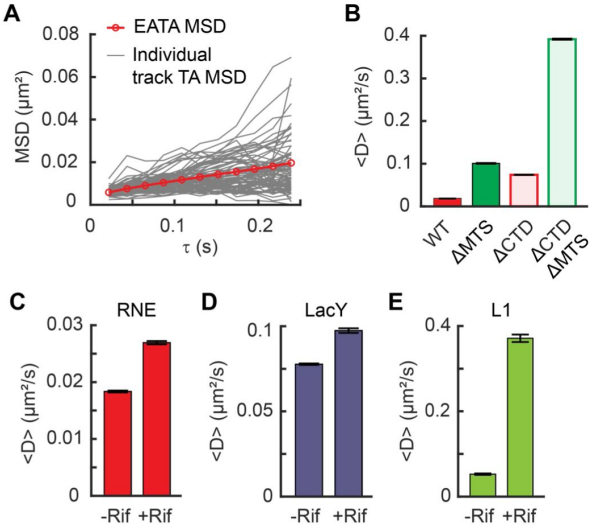

Diffusion of RNE in the absence of mRNA substrates

When some of RNE molecules interact with mRNA, their diffusion can slow due to the added mass of mRNA and ribosomes, possibly yielding slower RNE subpopulations. Such mobility-based subpopulations have been observed for RNA polymerases and ribosomes in *E. coli* and used to estimate the fraction of molecules interacting with RNA[35–37].

To test the effect of mRNA substrates on RNE diffusion, we treated cells with rifampicin (rif), which blocks transcription initiation, thus depleting cellular mRNAs[38]. In rif-treated cells, D_{RNE} increased to 0.0270 ± 0.0003 $\mu m^2/s$, which is 1.47 ± 0.010 times that in untreated cells (**Fig. 3C**). We note that D_{LacY} also increased to 1.25 ± 0.01 times relative to untreated cells (**Fig. 3D**). Although this increase is relatively small, the increase in D_{LacY} was unexpected because LacY is not an RNA-binding protein. The increase in D_{LacY} likely results from the depletion of mRNAs near the membrane (e.g., the mRNAs undergoing transertion), which could otherwise hinder the diffusion of membrane proteins[39,40]. The similar fold change in D_{RNE} and D_{LacY} upon rif treatment suggests that the change in RNE diffusion may largely be attributed to physical changes in the intracellular environment (such as reduced viscosity or macromolecular crowding[41,42]), rather than a loss of RNA-RNE interactions.

Because the rif-induced change in D_{RNE} is largely physical, we next examined why eliminating RNA-RNE interactions does not further increase RNE mobility, using the ribosome as a benchmark. The diffusion of ribosomal protein L1 became 7 times as fast as that in rif-treated cells (**Fig. 3E**), consistent with previous reports[35,36]. This big change can be explained by the fact that ribosomes form polysomes, where the effective mass of L1 protein in untreated cells would be 2 or more times that in rif-treated cells (where it remains as a free subunit). In the case of RNE, it forms the RNA degradosome complex, whose mass can be from 450 kDa[6] to 2.3 MDa depending on the occupancy of the RNA degradosome component proteins (RhlB, PNPase, enolase)[2,43–46] (**Supplementary Discussion)**. Even at its largest size, the RNE complex is smaller than a 70S ribosome (~2.5 MDa[47]). This means that if RNE interacts with an mRNA associated with n ribosomes, the total mass of the RNE complex would increase by a factor of n or more. Thus, a substantial increase in D_{RNE} would be expected upon mRNA depletion, assuming that a significant fraction of RNE is engaged with mRNA-ribosome assemblies.

To explain the marginal increase in D_{RNE} upon rif treatment, we considered two possibilities; (1) only a small percentage of RNE molecules interacts with mRNAs at a given time and/or (2) RNE interacts with mRNAs only briefly, unlike ribosomes which spend an order of 10-100 s in a polysome state during translation elongation[48]. To distinguish between these possibilities, we attempted to increase the cellular pool of polysomes, either by treating cells with a translation elongation inhibitor chloramphenicol[37] or by overexpressing *lacZ* mRNA from a high-copy plasmid (Fig. S3D-E). In both cases, a larger fraction of RNE would engage with mRNAs, potentially increasing the fraction of RNE in the slow-diffusing state. However, D_{RNE} remained unchanged compared to untreated cells (Fig. S3F). This result rules out the possibility that only a small percentage of RNE interacts with mRNAs and instead weighs in favor of the scenario that RNE-mRNA interactions are brief. Specifically, if RNE interacts with mRNAs for ~20 ms or less, the slow-diffusing state would last shorter than the frame interval and remain undetected in our experiment.

Diffusion and localization of the MTS and TM segments

Unlike RNE in *E. coli*, RNase Y, a functional homolog of RNE in *B. subtilis*, is localized to the membrane via a TM domain[20]. We wondered if there are differences between a peripheral motif (like the MTS of *E. coli*'s RNE) and a TM motif in terms of membrane localization and mobility. To address this question, we created RNE mutants in which the MTS was replaced with a

TM domain. For the TM domain, we used TM segments of LacY, a native *E. coli* protein, rather than using the TM motif from *B. subtilis* RNase Y, which might interact with the *E. coli* membrane in a non-native manner.

Before creating the RNE mutants, we characterized the MB% and the diffusion of individual short membrane-binding motifs. Native LacY contains 12 TM segments, arranged into two groups of six[28]. We successfully expressed constructs containing the first two TM segments (LacY (1-74) or LacY2), the first six TM segments (LacY (1-193) or LacY6), and the full-length LacY (LacY12), each fused to mEos3.2 and expressed from a chromosomal IPTG-inducible promoter (**Fig. 4A**). We then imaged their membrane localization and diffusion. Both the MTS segment and LacY-derived TM segments showed a strong membrane enrichment (**Fig. 4B**). In terms of diffusion, LacY2 and LacY6 diffused faster than the MTS segment (**Fig. 4C**), contrary to expectations based on size (or mass)-dependent diffusion (**Fig. 4D**).

According to the Stokes-Einstein relation for diffusion in simple fluids[49] and the Saffman-Delbruck diffusion model for membrane proteins[50], D decreases as particle size increases, albeit with different scaling behaviors. Specifically, the Saffman-Delbruck model predicts that D for membrane proteins decreases logarithmically with increasing radius of the membrane-embedded region, assuming a constant membrane environment[50]. Thus, if size (or mass) were the primary determinant of diffusion, LacY2 and LacY6 would diffuse more slowly than the smaller MTS. The observed discrepancy instead implies that D may be governed by how each motif interacts with the membrane. For example, the way that TM domains are anchored to the membrane may facilitate faster lateral diffusion with surrounding lipids.

Despite the prevalence of peripheral membrane proteins[51], how they interact with the membrane and how this differs from TM proteins remain poorly understood. To further explore this, we conducted all-atom molecular dynamics (MD) simulations of the MTS and the LacY variants interacting with the *E. coli* membrane using the NAMD software[52]. In the simulations, protein motion was calculated for 1 μs. Although the absolute D values were higher than experimental values (possibly due to the absence of mEos3.2 in the model), the overall trends were preserved; among the LacY series, larger constructs diffused more slowly (**Fig. 4E-F**, **Fig. S4A**). Most importantly, the MTS again diffused more slowly than LacY2 *in silico* (**Fig. 4E**, **Fig. S4A**). By calculating membrane-protein interaction energies, we found that the MTS-membrane interactions were more stable than those of LacY2 (**Fig. S4B**). These results suggest that the slower diffusion of the MTS is due to stronger interactions with lipid head groups compared to membrane-embedded TM segments.

RNE mutants carrying a TM motif

Since LacY2 and LacY6 showed strong membrane enrichment similar to LacY12 (**Fig. 4B**), we replaced the MTS in RNE with LacY2, LacY6, and LacY12 in the presence or absence of the CTD (**Fig. 5A-B** and **Fig. S5**). All chimeric RNE mutants were expressed from the native chromosomal locus as the only copy of *rne*, with mEos3.2 fused at the C terminus for imaging. The resulting strains exhibited no noticeable differences in growth rate compared to the WT strain (**Table S3**), suggesting that the RNE mutants were functionally active.

xNorm histograms of the ΔCTD mutants indicated membrane localization similar to LacY (**Fig. 5C**). However, mutants containing the CTD showed noticeable cytoplasmic subpopulations when LacY2 and LacY6 were used in place of the MTS (**Fig. 5D**, **Fig. S2J-K**, **Fig. S6B**). Mathematical model fitting of the xNorm histograms estimated the MB% of RNE-LacY2-CTD and RNE-LacY6-CTD to be 69% [66%, 73%] and 86% [84%, 90%], respectively (**Fig. 5F**). We note that imperfect membrane localization was observed only in mutants containing the CTD; the same protein without the CTD showed MB% of 100% (**Fig. 5E-F**, **Fig. S6A-B**). These findings suggest that the CTD may contribute to unstable membrane binding of RNE. Supporting this idea, previously characterized RNE MTS point mutants with MB% <50% (**Fig. 2D-E**) also exhibited

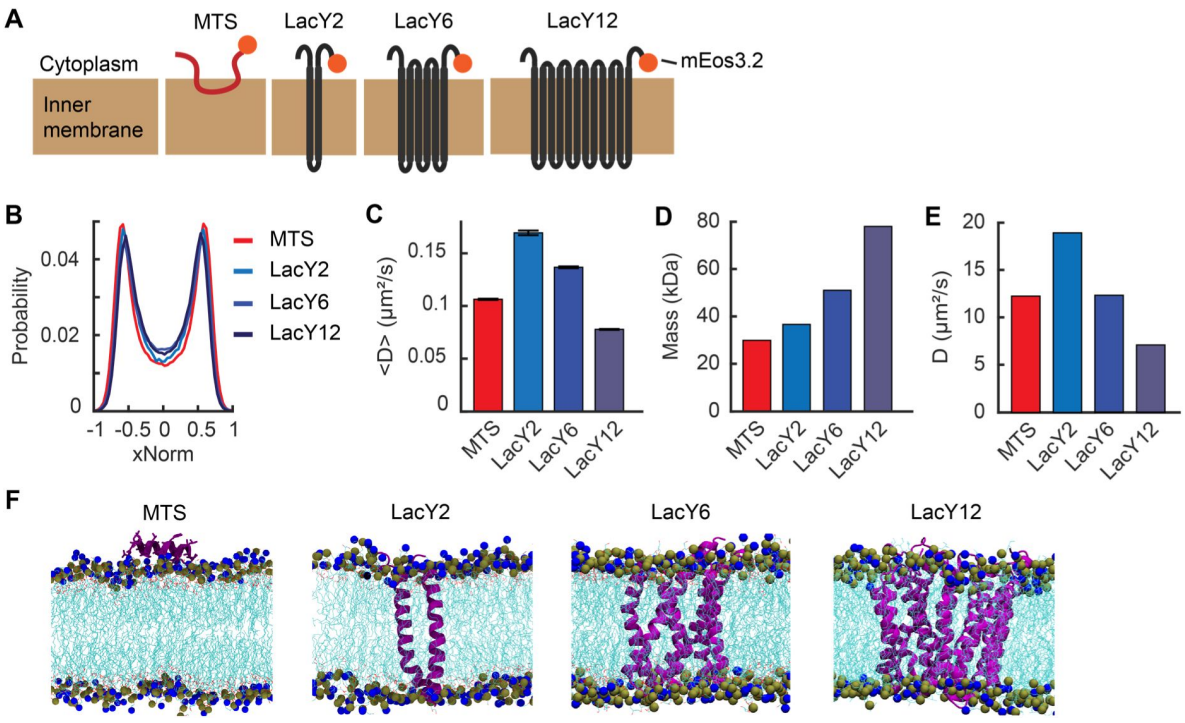

Figure 4

Localization and diffusion of membrane-binding motifs.

(**A**) Cartoon schematic of the membrane-binding motifs used in this study (not to scale). The orange circles indicate mEos3.2 used for imaging. (**B**) xNorm histograms of membrane-binding motifs. The SEM from bootstrapping is displayed but smaller than the line width. Data are from at least 107,000 spots. (**C**) Mean diffusion coefficients of membrane-binding motifs. Error bars are the SEM from at least 3,000 tracks. (**D**) Estimated mass of membrane-binding motifs based on the amino acid sequence including linkers and mEos3.2. (**E**) Diffusion coefficients of the membrane-binding motifs obtained from all-atom MD simulation. (**F**) Representative simulation snapshots of the membrane-binding motifs embedded in the *E. coli* membrane. Proteins are displayed in purple, and lipid tails are shown in cyan. Nitrogen and phosphorus atoms of the lipid head groups are represented in the van der Waals form in blue and grey, respectively. See **Table S6** for data statistics.

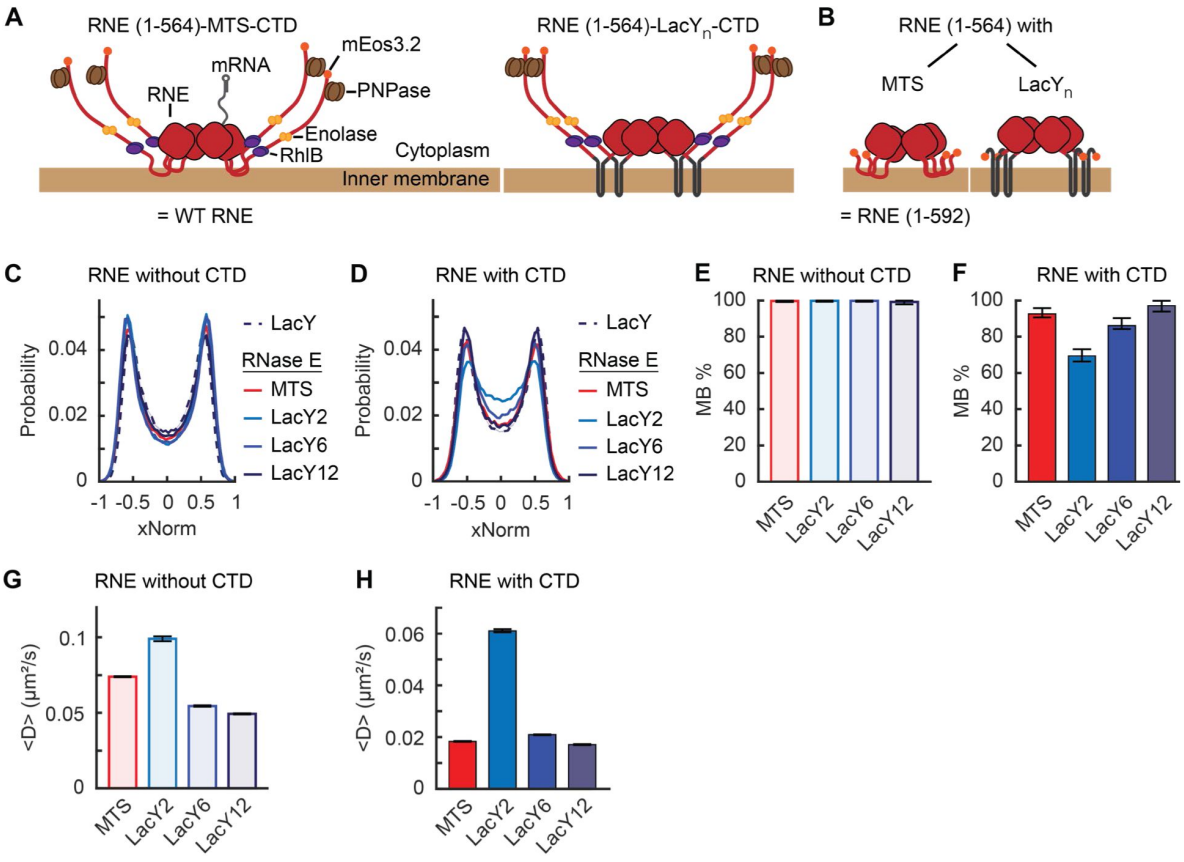

Figure 5

Localization and diffusion of chimeric RNE with or without the CTD.

(**A-B**) Cartoon schematic of RNE chimeric variants with the CTD (**A**) and without the CTD (**B**). They are not to scale. (**C-D**) xNorm histograms of chimeric RNE localization compared with that of LacY. The SEM from bootstrapping is displayed but smaller than the line width. (**E-F**) MB% of chimeric RNE mutants without the CTD (**E**) or with the CTD (**F**) with various membrane-binding motifs. Error bars are from a 95% confidence interval. (**G-H**) Mean diffusion coefficients of chimeric RNE without the CTD (**G**) or with the CTD (**H**). Error bars are the SEM. Each data set contains at least 70,000 tracks for diffusion or 72,000 spots for xNorm. See **Table S6** for data statistics.

increased MB% upon the CTD removal (**Fig. S6A-B**). Such a difference in MB% between the CTD-containing and the CTD-lacking mutants was not observed in the chimera based on LacY12 (**Fig. 5E-F**), possibly due to the stable membrane insertion by LacY12.

Next, we examined whether the *D* of chimeric RNE mutants varied depending on the type of membrane-binding motifs. For example, the MTS diffused more slowly than LacY2 and LacY6, despite being smaller in size (**Fig. 4C-D**). Based on this, we expected the chimeric RNE with LacY2 or LacY6 to diffuse faster than RNE with MTS. Indeed, in the absence of the CTD, we found that the *D* of LacY2-based RNE was 1.33 ± 0.01 times as fast as the MTS-based RNE (**Fig. 5G**). However, LacY6-based RNE did not diffuse faster than the MTS-based version (**Fig. 5G**). This result may be due to the high TM load (24 helices) created by four LacY6 anchors in the RNE tetramer. Although all constructs are tetrameric, the 24-helix load (LacY6), compared with 8 (LacY2) and 4 (MTS), likely enlarges the membrane-embedded footprint and increases drag, thereby changing the mobility advantages assessed as standalone membrane anchors.

In the presence of the CTD, the *D* of LacY2 and LacY6-based RNE became 3.33 ± 0.004 and 1.14 ± 0.01 times that of the MTS-based RNE counterpart (i.e. the WT RNE), respectively (**Fig. 5H**). This is likely influenced by the presence of a cytoplasmic population (~31% for LacY2 and ~14% for LacY6; **Fig. 5F**, **Fig S2J-K**), which diffuses more rapidly than membrane-bound molecules (possibly by a factor of five, based on **Fig. 3B**). Taken together, our data suggest that the CTD weakens the membrane association of RNE and small TM motifs can facilitate the diffusion of RNE.

Functional consequence of subcellular localization and diffusion of RNE

To check the functional consequence of cytoplasmic localization of RNE, we measured *lacZ* mRNA degradation in various RNE mutants presented in this study. Recently, we developed an assay to quantify both co-transcriptional and post-transcriptional degradation rates of *lacZ* mRNA by inducing its transcription for only 75 s, thereby capturing the degradation of nascent mRNA[15]. In WT cells, we found that the co-transcriptional degradation rate (k_{d1}) is about 10 times slower than the post-transcriptional degradation rate (k_{d2})[15]. In cells expressing RNE ΔMTS, however, k_{d1} increases by a factor of ~3, suggesting that cytoplasmic RNE can freely diffuse and degrade nascent mRNAs[15]. This result led us to hypothesize that RNE variants exhibiting a cytoplasmic subpopulation (**Fig. 2E** and **5F**) may exhibit a larger k_{d1} compared to more membrane-bound variants.

We repeated this assay in a strain expressing the WT RNE fused to mEos3.2 (**Fig. S7A**). Note that this strain is different from the one we used for imaging because a monocistronic *lacZ* gene is needed for the transient induction assay[15]. The relative abundances of 5' *lacZ* mRNA (Z5) remained constant prior to the rise in 3' *lacZ* mRNA (Z3) levels (between ~100 and 210 s), confirming negligible co-transcriptional degradation in WT cells[15] (**Fig. 6A**). However, in cells expressing RNE-LacY2-CTD (MB% = 69%), Z5 levels exhibited a downward trend during the same time window (**Fig. 6B**). The estimated k_{d1} was close to what was observed in RNE ΔMTS[15] (gray line, p = 0.28; **Fig. 6C**). A similarly high k_{d1} was also observed in RNE MTS point mutations, F582E and F757E, which exhibited a ΔMTS-like xNorm profile (**Fig. 2D**), supporting the idea that the cytoplasmic subpopulation of RNE enables co-transcriptional mRNA degradation in *E. coli* (**Fig. 6C**). Notably, RNE-LacY6-CTD, which also exhibited a cytoplasmic subpopulation (~14% from MB% of 86%), did not exhibit a significant increase in k_{d1} (**Fig. 6C**), suggesting a critical amount of cytoplasmic population may be needed to facilitate co-transcriptional mRNA degradation

We next examined whether the post-transcriptional mRNA degradation rate (k_{d2}) is limited by the slow diffusion of membrane-bound RNE. In the presence of the CTD, k_{d2} did not significantly vary across membrane-targeting variants (**Fig. 6D**). For example, even though the LacY12 motif slows RNE diffusion, its $k_{d\,2}$ was similar to that of WT RNE (**Fig. 6D**). A critical control for this

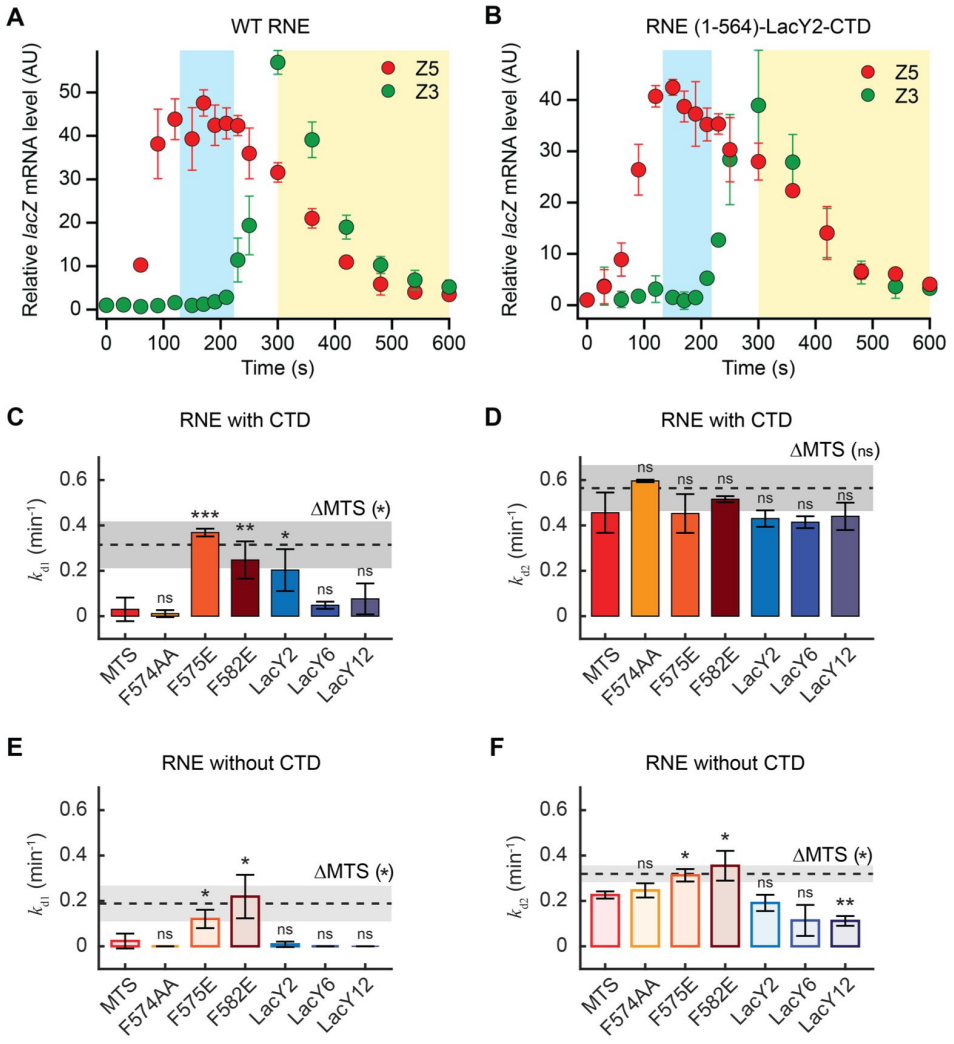

Figure 6

lacZ mRNA degradation rates in RNE mutant strains.

(**A-B**) *lacZ* mRNA levels in WT RNE (**A**, strain SK595) and in RNE-LacY2-CTD (**B**, strain SK505) when *lacZ* transcription was induced with 0.2 mM IPTG at t = 0 s and re-repressed with 500 mM glucose at t = 75 s. Blue and yellow regions indicate the time windows used to measure k_{d1} and k_{d2}, respectively, by exponential fitting of 5' *lacZ* mRNA (Z5) in individual replicates. (**C-F**) Co-transcriptional and post-transcriptional *lacZ* mRNA degradation rates, k_{d1} (**C, E**) and k_{d2} (**D, F**), respectively, in various RNE mutants containing different membrane-binding motifs, either with the CTD (solid bars, **C-D**) or ΔCTD (light bars, **E-F**). The dotted lines indicate the k_{d1} and k_{d2} values of cytoplasmic RNE ΔMTS (strain SK339 in **C-D**)$_{15}$ or RNE ΔMTS ΔCTD (strain SK370, in **E-F**). In all panels, error bars represent the standard deviations from 2-3 biological replicates. Two-sample *t*-tests were performed relative to the MTS case in each graph (See **Table S7** for the *p* values).

comparison is RNE abundance: because RNE autoregulates its expression by degrading its own transcript[53], slower diffusion could elevate RNE levels and mask the negative effect of the reduced mobility. We tested this explicitly and found that over-expression of WT RNE does not significantly change k_{d1} or k_{d2} (Fig. S7B). Thus, when the CTD is present, neither copy number nor diffusion of membrane-bound RNE limits k_{d2}.

In the absence of the CTD, k_{d1} was high in RNE variant F582E (MB% = 67%; Fig. S6A), reaching levels close to its cytoplasmic counterpart, the ΔMTS ΔCTD mutant (gray line, p = 0.7; **Fig. 6E**). k_{d2} values for ΔCTD variants were, in general, lower than those of their CTD-containing counterparts (**Fig. 6F**), indicating the importance of the CTD for the catalytic activity. These findings are consistent with previous reports on RNE constructs based on the MTS[15,22–24]. Among ΔCTD variants with different membrane motifs, point mutants F575E and F582E (MB% = 91% and 67%, respectively; Fig. S6A) exhibited higher k_{d2} than the MTS-based variant, in agreement with the fact that completely cytoplasmic ΔMTS ΔCTD exhibited higher k_{d2} than the MTS-containing ΔCTD (**Fig. 6F**). However, the LacY2-based RNE variant, which diffuses faster than the MTS version (**Fig. 5G**), did not show a corresponding increase in k_{d2} (**Fig. 6F**). Plus, LacY6 and LacY12 versions showed even lower k_{d2} than MTS-based RNE ΔCTD. Overall, these results indicate that the reduced k_{d2} caused by ΔCTD cannot be rescued by faster diffusion of membrane-bound RNE. In fact, it may be further impaired by large and slow membrane motifs (such as LacY12). The presence of the CTD appears to buffer the effects of large membrane-binding motifs on RNE's catalytic activity, helping to maintain efficient post-transcriptional mRNA degradation (k_{d2}).

Discussion

Our study establishes the membrane enrichment and slow diffusion of RNE in *E. coli*. This supports the notion that sequestration of RNE on the membrane confers the spatial and temporal separation between synthesis and decay of mRNAs[15]. Furthermore, the processing of rRNA[54–58] and tRNA[59,60] and small RNA-based gene regulations[61,62] mediated by RNE likely take place on the membrane.

For WT RNE, our analysis showed MB% of 93%, close to 91% previously reported using immunogold labeling and freeze-fracture electron microscopy[63]. Whether the MB% of RNE changes under different growth conditions remains to be tested. As a case study, we examined the MB% of WT RNE when cells were grown in M9 minimal medium with succinate as the sole carbon source without supplements, a condition different from that used in our primary experiments (M9 glycerol with supplements). The MTS segment exhibited a reduction in MB% from 100% to 83% (Fig. S6C), suggesting that MTS-mediated membrane binding can be sensitive to growth conditions. However, the MB% of WT RNE was only marginally affected by the same media change (Fig. S6C). We speculate that tetramer formation stabilizes RNE membrane localization, even when individual MTS motifs exhibit a weak membrane affinity. A similar phenomenon has been observed with MinD; although its amphipathic motif alone is cytoplasmic, MinD becomes membrane-associated upon dimerization, indicating that oligomerization enhances the membrane binding of this peripheral membrane protein[64]. By analogy, the tetrameric structure of RNE may reinforce membrane association, buffering against changes in cellular metabolism or lipid environment that would otherwise weaken MTS-mediated binding.

While individual TM motifs exhibited strong membrane association regardless of growth conditions (Fig. S6D), we found LacY2-based RNE can lose membrane binding affinity, unlike MTS-based RNE. The loss of MB% in LacY2-based RNE was observed only in the presence of the CTD (Fig. S6D), suggesting that the CTD negatively affects membrane binding of RNE, possibly by altering protein conformation. In fact, all ΔCTD RNE mutants we tested exhibited higher MB% than their CTD-containing counterparts (Fig. S6A-B). For example, WT RNE (containing CTD) showed

an MB% of 93%, whereas its ΔCTD version, RNE (1-592), showed 100%. Similarly, the chimeric RNE-LacY6-CTD showed an MB% of 86%, while its ΔCTD version showed 100% (**Fig. 5E-F**, **Fig. S6A-B**). A similar trend was observed for MTS point mutants (**Fig. S6A-B**), further supporting that the CTD decreases membrane association across RNE variants. We speculate that this effect may be related to the CTD's role in promoting phase-separated ribonucleoprotein condensates, as observed in *Caulobacter crescentus*[19]. In *E. coli*, we also observed a modest increase in the clustering tendency of RNE compared to ΔCTD (Fig. S8).

The D_{RNE} we measured in *E. coli* (0.018 $\mu m^2/s$) is comparable to those measured in other bacterial species. For example, in *C. crescentus*, the *D* of its cytoplasmic RNE was shown to be about 0.03 $\mu m^2/s$[65]. The diffusion of RNase Y in *B. subtilis* was found in either a slow (0.031 $\mu m^2/s$) or fast (0.3 $\mu m^2/s$) population[66], with the slow population corresponding to RNase Y bound to mRNA and/or the putative RNA degradosome and the fast population representing freely diffusing RNase Y. In the case of *E. coli* RNE, a two-population fit of the *D* histogram based on MB% identified the slow and fast subpopulations whose *D* values differed by a factor of 4 (Fig. S3C). This agrees with our finding that cytoplasmic RNE ΔMTS diffuses ~5 times as fast as WT RNE on average (**Fig. 3B**).

Diffusion is affected by the size of the particle in a given medium[50], and it has been used to identify different size forms of a protein due to biochemical interactions or complex formation[36,67]. Related, RNA substrates interacting with RNE can also increase the effective mass of RNE and lower its *D* value. However, when cellular mRNAs were depleted by rifampicin treatment, RNE diffusion increased less than that of other RNA-binding proteins related to transcription and translation. For example, the large and small ribosomal subunits[35,36,68], tRNA[69], and RNA polymerase[37] showed a large (about 10-20 fold) increase in *D* upon rifampicin treatment. Interestingly, Hfq, an RNA chaperon involved in small RNA regulation together with RNE, showed a moderate increase (~2 fold) in *D* when RNA was depleted by rifampicin[70]. We note that our result is consistent with previous studies that examined the effect of rifampicin on RNE diffusion in *E. coli*[11,71] as well as RNE in *C. crescentus*[65] and RNase Y in *B. subtilis*[66,72]. One possible explanation is that RNA-bound RNE (and RNase Y) is short-lived compared to our frame interval (~20 ms), unlike other RNA-binding proteins related to transcription and translation, interacting with RNA for ~1 min for elongation[48].

Lastly, the slow diffusion of the MTS in comparison to LacY2 and LacY6 suggests that MTS is less favorable for rapid lateral motion in the membrane. Our MD simulations demonstrated that this reduced diffusivity may originate from a stronger interaction energy between the protein and the membrane. Whether this property is specific to the MTS or generalizable to other peripheral versus integral membrane motifs remains to be tested. We speculate that this can be a general phenomenon, as peripheral motifs interact with lipids orthogonally while integral membrane motifs align parallel to the bilayer and may diffuse more freely by coupling with the motion of surrounding lipids. The diffusion behavior of membrane-bound proteins reflects underlying protein-lipid interactions and membrane dynamics[73]. Accordingly, future work may analyze how protein-lipid interaction strength and membrane dynamics contribute to differences in lateral diffusion between peripheral and integral membrane proteins.

Altogether, our work highlights strategies to modulate the MB% and diffusion of RNE to possibly affect mRNA degradation rates. For example, membrane-bound RNE lacking the CTD can stabilize mRNAs and increase protein expression. This idea has been used in a commercial *E. coli* BL21 strain (Invitrogen's One Shot BL21 Star) to increase recombinant protein yield[22]. Additionally, RNE variants with environmentally responsive MB%, such as RNE-LacY2-CTD, could be harnessed to tune mRNA half-lives and protein expression levels under different growth conditions.

Acknowledgements

We thank Drs. Mark Arbing, Agamemnon Carpousis, Johan Elf, and Christine Jacobs-Wagner for strains. We thank Maggie Liu, Kavya Vaidya, and Zach Wang for their contributions in the early phase of this work and the members of Kim lab for critical reading of the manuscript. This work was supported by the NSF Center for Physics of Living Cells (1430124), NSF Science and Technology Center for Quantitative Cell Biology (2243257), NIH (R35GM143203; R24GM145965), and Searle Scholars Program.

Additional information

Author contributions

L.T. and S.K. designed the research; L.T. and Y.W. performed imaging and analysis; L.T. and Se.K. measured mRNA lifetimes; LT, Se.K., and S.K. performed genetics; L.T., Y.W., and J.W. developed data analysis methods; S. performed all-atom MD simulations under supervision of E.T.; B.R. performed epi-fluorescence imaging; L.T. and S.K. wrote the manuscript with input from all authors; S.K. supervised the study.

Funding

NIH (R35GM143203)

NIH (R24GM145965)

NSF (2243257)

NSF (1430124)

Additional files

Supplemental Information

References

1 Mudd E. A., Krisch H. M., Higgins C. F (1990) **RNase E, an endoribonuclease, has a general role in the chemical decay of Escherichia coli mRNA: evidence that rne and ams are the same genetic locus** *Molecular Microbiology* **4**:2127–2135 https://doi.org/10.1111/j.1365-2958.1990.tb00574.x | Google Scholar

2 Mackie G. A (2013) **RNase E: at the interface of bacterial RNA processing and decay** *Nature Reviews Microbiology* **11**:45–57 https://doi.org/10.1038/nrmicro2930 | Google Scholar

3 Hui M. P., Foley P. L., Belasco J. G (2014) **Messenger RNA degradation in bacterial cells** *Annual Review of Genetics* **48**:537–559 https://doi.org/10.1146/annurev-genet-120213-092340 | Google Scholar

4 Apirion D., Lassar A. B (1978) **A conditional lethal mutant of Escherichia coli which affects the processing of ribosomal RNA** *Journal of Biological Chemistry* **253**:1738–1742 https://doi.org/10.1016/S0021-9258(17)34927-X | Google Scholar

5 Babitzke P., Kushner S. R (1991) **The Ams (altered mRNA stability) protein and ribonuclease E are encoded by the same structural gene of Escherichia coli** *Proceedings of the National Academy of Sciences* **88**:1–5 https://doi.org/10.1073/pnas.88.1.1 | Google Scholar

6 Carpousis A. J (2007) **The RNA degradosome of Escherichia coli: an mRNA-degrading machine assembled on RNase E** *Annual Review of Microbiology* **61**:71–87 https://doi.org/10.1146/annurev.micro.61.080706.093440 | Google Scholar

7 Aït-Bara S., Carpousis A. J (2015) **RNA degradosomes in bacteria and chloroplasts: classification, distribution and evolution of RNase E homologs** *Molecular Microbiology* **97**:1021–1135 https://doi.org/10.1111/mmi.13095 | Google Scholar

8 Mardle C. E., et al. (2019) **A structural and biochemical comparison of ribonuclease E homologues from pathogenic bacteria highlights species-specific properties** *Scientific Reports* **9**:7952 https://doi.org/10.1038/s41598-019-44385-y | Google Scholar

9 Callaghan A. J., et al. (2005) **Structure of Escherichia coli RNase E catalytic domain and implications for RNA turnover** *Nature* **437**:1187–1191 https://doi.org/10.1038/nature04084 | Google Scholar

10 Khemici V., Poljak L., Luisi B. F., Carpousis A. J (2008) **The RNase E of Escherichia coli is a membrane-binding protein** *Molecular Microbiology* **70**:799–813 https://doi.org/10.1111/j.1365-2958.2008.06454.x | Google Scholar

11 Strahl H., et al. (2015) **Membrane recognition and dynamics of the RNA degradosome** *PLOS Genetics* **11**:e1004961 https://doi.org/10.1371/journal.pgen.1004961 | Google Scholar

12 Kaberdin V. R., et al. (1998) **The endoribonucleolytic N-terminal half of Escherichia coli RNase E is evolutionarily conserved in Synechocystis sp. and other bacteria but not the C-terminal half, which is sufficient for degradosome assembly** *Proceedings of the National Academy of Sciences* **95**:11637–11642 https://doi.org/10.1073/pnas.95.20.11637 | Google Scholar

13 Lee K., Cohen S. N (2003) **A Streptomyces coelicolor functional orthologue of Escherichia coli RNase E shows shuffling of catalytic and PNPase-binding domains** *Molecular Microbiology* **48**:349–360 https://doi.org/10.1046/j.1365-2958.2003.03435.x | Google Scholar

14 Hadjeras L., et al. (2019) **Detachment of the RNA degradosome from the inner membrane of Escherichia coli results in a global slowdown of mRNA degradation, proteolysis of RNase E and increased turnover of ribosome-free transcripts** *Molecular Microbiology* **111**:1715–1731 https://doi.org/10.1111/mmi.14248 | Google Scholar

15 Kim S., Wang Y.-H., Hassan A., Kim S (2024) **Re-defining how mRNA degradation is coordinated with transcription and translation in bacteria** *bioRxiv* https://doi.org/10.1101/2024.04.18.588412 | Google Scholar

16 Moffitt J. R., Pandey S., Boettiger A. N., Wang S., Zhuang X (2016) **Spatial organization shapes the turnover of a bacterial transcriptome** *eLife* **5**:e13065 https://doi.org/10.7554/eLife.13065 | Google Scholar

17 Murashko O. N., Lin-Chao S (2017) **Escherichia coli responds to environmental changes using enolasic degradosomes and stabilized DicF sRNA to alter cellular morphology** *Proceedings of the National Academy of Sciences* **114**:E8025–E8034 https://doi.org/10.1073/pnas.1703731114 | Google Scholar

18 Gohrbandt M., et al. (2022) **Low membrane fluidity triggers lipid phase separation and protein segregation in living bacteria** *The EMBO Journal* **41**:e109800 https://doi.org/10.15252/embj.2021109800 | Google Scholar

19 Al-Husini N., Tomares D. T., Bitar O., Childers W. S., Schrader J. M (2018) **α-Proteobacterial RNA degradosomes assemble liquid-liquid phase-separated RNP bodies** *Molecular Cell* **71**:1027–1039 https://doi.org/10.1016/j.molcel.2018.08.003 | Google Scholar

20 Lehnik-Habrink M., et al. (2011) **RNase Y in Bacillus subtilis: a natively disordered protein that is the functional equivalent of RNase E from Escherichia coli** *Journal of Bacteriology* **193**:5431–5441 https://doi.org/10.1128/jb.05500-11 | Google Scholar

21 Callaghan A. J., et al. (2004) **Studies of the RNA degradosome-organizing domain of the Escherichia coli ribonuclease RNase E** *Journal of Molecular Biology* **340**:965–979 https://doi.org/10.1016/j.jmb.2004.05.046 | Google Scholar

22 Lopez P. J., Marchand I., Joyce S. A., Dreyfus M (1999) **The C-terminal half of RNase E, which organizes the Escherichia coli degradosome, participates in mRNA degradation but not rRNA processing in vivo** *Molecular Microbiology* **33**:188–199 https://doi.org/10.1046/j.1365-2958.1999.01465.x | Google Scholar

23 Leroy A., Vanzo N. F., Sousa S., Dreyfus M., Carpousis A. J (2002) **Function in Escherichia coli of the non-catalytic part of RNase E: role in the degradation of ribosome-free mRNA** *Molecular Microbiology* **45**:1231–1243 https://doi.org/10.1046/j.1365-2958.2002.03104.x | Google Scholar

24 Islam M. S., Bandyra K. J., Chao Y., Vogel J., Luisi B. F (2021) **Impact of pseudouridylation, substrate fold, and degradosome organization on the endonuclease activity of RNase E** *RNA* **27**:1339–1352 https://doi.org/10.1261/rna.078840.121 | Google Scholar

25 Zhang M., et al. (2012) **Rational design of true monomeric and bright photoactivatable fluorescent proteins** *Nature Methods* **9**:727–729 https://doi.org/10.1038/nmeth.2021 | Google

Scholar

26 Jaqaman K., et al. (2008) **Robust single-particle tracking in live-cell time-lapse sequences** *Nature Methods* **5**:695–702 https://doi.org/10.1038/nmeth.1237 | Google Scholar

27 Paintdakhi A., et al. (2016) **Oufti: an integrated software package for high-accuracy, high-throughput quantitative microscopy analysis** *Molecular Microbiology* **99**:767–777 https://doi.org/10.1111/mmi.13264 | Google Scholar

28 Abramson J., et al. (2003) **Structure and mechanism of the lactose permease of Escherichia coli** *Science* **301**:610–615 https://doi.org/10.1126/science.1088196 | Google Scholar

29 Ahrem B., Hoffschulte H. K., Müller M (1989) **In vitro membrane assembly of a polytopic, transmembrane protein results in an enzymatically active conformation** *J Cell Biol* **108**:1637–1646 https://doi.org/10.1083/jcb.108.5.1637 | Google Scholar

30 Nagamori S., Vázquez-Ibar J. L., Weinglass A. B., Kaback H. R (2003) **In vitro synthesis of lactose permease to probe the mechanism of membrane insertion and folding** *Journal of Biological Chemistry* **278**:14820–14826 https://doi.org/10.1074/jbc.M300332200 | Google Scholar

31 Stochaj U., Ehring R (1987) **The N-terminal region of Escherichia coli lactose permease mediates membrane contact of the nascent polypeptide chain** *European Journal of Biochemistry* **163**:653–658 https://doi.org/10.1111/j.1432-1033.1987.tb10914.x | Google Scholar

32 Volkov I. L., et al. (2022) **Spatiotemporal kinetics of the SRP pathway in live E. coli cells** *Proceedings of the National Academy of Sciences* **119**:e2204038119 https://doi.org/10.1073/pnas.2204038119 | Google Scholar

33 Thappeta Y., et al. (2024) **Glycogen phase separation drives macromolecular rearrangement and asymmetric division in E. coli** *bioRxiv* https://doi.org/10.1101/2024.04.19.590186 | Google Scholar

34 Savin T., Doyle P. S (2005) **Static and dynamic errors in particle tracking microrheology** *Biophysical Journal* **88**:623–638 https://doi.org/10.1529/biophysj.104.042457 | Google Scholar

35 Bakshi S., Siryaporn A., Goulian M., Weisshaar J. C (2012) **Superresolution imaging of ribosomes and RNA polymerase in live Escherichia coli cells** *Molecular Microbiology* **85**:21–38 https://doi.org/10.1111/j.1365-2958.2012.08081.x | Google Scholar

36 Sanamrad A., et al. (2014) **Single-particle tracking reveals that free ribosomal subunits are not excluded from the Escherichia coli nucleoid** *Proceedings of the National Academy of Sciences* **111**:11413–11418 https://doi.org/10.1073/pnas.1411558111 | Google Scholar

37 Stracy M., et al. (2015) **Live-cell superresolution microscopy reveals the organization of RNA polymerase in the bacterial nucleoid** *Proceedings of the National Academy of Sciences* **112**:E4390–E4399 https://doi.org/10.1073/pnas.1507592112 | Google Scholar

38 Mosteller R. D., Yanofsky C (1970) **Transcription of the tryptophan operon in Escherichia coli: Rifampicin as an inhibitor of initiation** *Journal of Molecular Biology* **48**:525–531 https://doi.org/10.1016/0022-2836(70)90064-1 | Google Scholar

39 Binenbaum Z., Parola A. H., Zaritsky A., Fishov I (1999) **Transcription- and translation-dependent changes in membrane dynamics in bacteria: testing the transertion model for**

domain formation *Molecular Microbiology* **32**:1173–1182 https://doi.org/10.1046/j.1365-2958.1999.01426.x | Google Scholar

40 Matsumoto K., Hara H., Fishov I., Mileykovskaya E., Norris V (2015) **The membrane: transertion as an organizing principle in membrane heterogeneity** *Frontiers in Microbiology* **6**:572 https://doi.org/10.3389/fmicb.2015.00572 | Google Scholar

41 Bellotto N., et al. (2022) **Dependence of diffusion in Escherichia coli cytoplasm on protein size, environmental conditions, and cell growth** *eLife* **11**:e82654 https://doi.org/10.7554/eLife.82654 | Google Scholar

42 Linnik D., Maslov I., Punter C. M., Poolman B (2024) **Dynamic structure of E. coli cytoplasm: supramolecular complexes and cell aging impact spatial distribution and mobility of proteins** *Communications Biology* **7**:508 https://doi.org/10.1038/s42003-024-06216-3 | Google Scholar

43 Chandran V., Luisi B. F (2006) **Recognition of enolase in the Escherichia coli RNA degradosome** *Journal of Molecular Biology* **358**:8–15 https://doi.org/10.1016/j.jmb.2006.02.012 | Google Scholar

44 Chandran V., et al. (2007) **Recognition and cooperation between the ATP-dependent RNA helicase RhlB and ribonuclease RNase E** *Journal of Molecular Biology* **367**:113–132 https://doi.org/10.1016/j.jmb.2006.12.014 | Google Scholar

45 Nurmohamed S., McKay A. R., Robinson C. V., Luisi B. F (2010) **Molecular recognition between Escherichia coli enolase and ribonuclease E** *Acta Crystallographica Section D* **66**:1036–1040 https://doi.org/10.1107/S0907444910030015 | Google Scholar

46 Nurmohamed S., Vaidialingam B., Callaghan A. J., Luisi B. F (2009) **Crystal structure of Escherichia coli polynucleotide phosphorylase core bound to RNase E, RNA and manganese: implications for catalytic mechanism and RNA degradosome assembly** *Journal of Molecular Biology* **389**:17–33 https://doi.org/10.1016/j.jmb.2009.03.051 | Google Scholar

47 Stark H., et al. (1995) **The 70S Escherichia coli ribosome at 23 å resolution: fitting the ribosomal RNA** *Structure* **3**:815–821 https://doi.org/10.1016/S0969-2126(01)00216-7 | Google Scholar

48 Dai X., et al. (2016) **Reduction of translating ribosomes enables Escherichia coli to maintain elongation rates during slow growth** *Nature Microbiology* **2**:16231 https://doi.org/10.1038/nmicrobiol.2016.231 | Google Scholar

49 Miller C. C., Walker J (1924) **The Stokes-Einstein law for diffusion in solution. Proceedings of the Royal Society of London. Series A** *Containing Papers of a Mathematical and Physical Character* **106**:724–749 https://doi.org/10.1098/rspa.1924.0100 | Google Scholar

50 Saffman P. G., Delbrück M (1975) **Brownian motion in biological membranes** *Proceedings of the National Academy of Sciences* **72**:3111–3113 https://doi.org/10.1073/pnas.72.8.3111 | Google Scholar

51 Papanastasiou M., et al. (2013) **The Escherichia coli peripheral inner membrane proteome** *Molecular & Cellular Proteomics* **12**:599–610 https://doi.org/10.1074/mcp.M112.024711 | Google Scholar

52 Phillips J. C., et al. (2005) **Scalable molecular dynamics with NAMD** *Journal of Computational Chemistry* **26**:1781–1802 https://doi.org/10.1002/jcc.20289 | Google Scholar

53 Schuck A., Diwa A., Belasco J. G (2009) **RNase E autoregulates its synthesis in Escherichia coli by binding directly to a stem-loop in the rne 5' untranslated region** *Molecular Microbiology* **72**:470–478 https://doi.org/10.1111/j.1365-2958.2009.06662.x | Google Scholar

54 Apirion D (1978) **Isolation, genetic mapping and some characterization of a mutation in Escherichia coli that affects the processing of ribonucleic acid** *Genetics* **90**:659–671 https://doi.org/10.1093/genetics/90.4.659 | Google Scholar

55 Bessarab D. A., Kaberdin V. R., Wei C.-L., Liou G.-G., Lin-Chao S (1998) **RNA components of Escherichia coli degradosome: evidence for rRNA decay** *Proceedings of the National Academy of Sciences* **95**:3157–3161 https://doi.org/10.1073/pnas.95.6.3157 | Google Scholar

56 Ghora B. K., Apirion D (1978) **Structural analysis and in vitro processing to p5 rRNA of a 9S RNA molecule isolated from an rne mutant of E. coli** *Cell* **15**:1055–1066 https://doi.org/10.1016/0092-8674(78)90289-1 | Google Scholar

57 Li Z., Pandit S., Deutscher M. P (1999) **RNase G (CafA protein) and RNase E are both required for the 5' maturation of 16S ribosomal RNA** *The EMBO Journal* **18**:2878–2885 https://doi.org/10.1093/emboj/18.10.2878 | Google Scholar

58 Roy M. K., Singh B., Ray B. K., Apirion D (1983) **Maturation of 5-S rRNA: ribonuclease E cleavages and their dependence on precursor sequences** *European Journal of Biochemistry* **131**:119–127 https://doi.org/10.1111/j.1432-1033.1983.tb07238.x | Google Scholar

59 Li Z., Deutscher M. P (2002) **RNase E plays an essential role in the maturation of Escherichia coli tRNA precursors** *RNA* **8**:97–109 Google Scholar

60 Ow M. C., Kushner S. R (2002) **Initiation of tRNA maturation by RNase E is essential for cell viability in E. coli** *Genes & Development* **16**:1102–1115 https://doi.org/10.1101/gad.983502 | Google Scholar

61 Ikeda Y., Yagi M., Morita T., Aiba H (2011) **Hfq binding at RhlB-recognition region of RNase E is crucial for the rapid degradation of target mRNAs mediated by sRNAs in Escherichia coli** *Molecular Microbiology* **79**:419–432 https://doi.org/10.1111/j.1365-2958.2010.07454.x | Google Scholar

62 Reyer M. A., et al. (2021) **Kinetic modeling reveals additional regulation at co-transcriptional level by post-transcriptional sRNA regulators** *Cell Reports* **36**:109764 https://doi.org/10.1016/j.celrep.2021.109764 | Google Scholar

63 Liou G.-G., Jane W.-N., Cohen S. N., Lin N.-S., Lin-Chao S (2001) **RNA degradosomes exist in vivo in Escherichia coli as multicomponent complexes associated with the cytoplasmic membrane via the N-terminal region of ribonuclease E** *Proceedings of the National Academy of Sciences* **98**:63–68 https://doi.org/10.1073/pnas.98.1.63 | Google Scholar

64 Szeto T. H., Rowland S. L., Habrukowich C. L., King G. F (2003) **The MinD membrane targeting sequence is a transplantable lipid-binding helix** *Journal of Biological Chemistry* **278**:40050–

40056 https://doi.org/10.1074/jbc.M306876200 | Google Scholar

65 Bayas C. A., et al. (2018) **Spatial organization and dynamics of RNase E and ribosomes in Caulobacter crescentus** *Proceedings of the National Academy of Sciences* **115**:E3712–E3721 https://doi.org/10.1073/pnas.1721648115 | Google Scholar

66 Oviedo-Bocanegra L. M., Hinrichs R., Rotter, Daniel Andreas O., Dersch S., Graumann P. L. (2021) **Single molecule/particle tracking analysis program SMTracker 2.0 reveals different dynamics of proteins within the RNA degradosome complex in Bacillus subtilis** *Nucleic Acids Research* **49**:e112–e112 https://doi.org/10.1093/nar/gkab696 | Google Scholar

67 Kapanidis A. N., Uphoff S., Stracy M (2018) **Understanding protein mobility in bacteria by tracking single molecules** *Journal of Molecular Biology* **430**:4443–4455 https://doi.org/10.1016/j.jmb.2018.05.002 | Google Scholar

68 Gray W. T., et al. (2019) **Nucleoid size scaling and intracellular organization of translation across bacteria** *Cell* **177**:1632–1648 https://doi.org/10.1016/j.cell.2019.05.017 | Google Scholar

69 Volkov I. L., et al. (2018) **tRNA tracking for direct measurements of protein synthesis kinetics in live cells** *Nature Chemical Biology* **14**:618–626 https://doi.org/10.1038/s41589-018-0063-y | Google Scholar

70 Park S., et al. (2021) **Dynamic interactions between the RNA chaperone Hfq, small regulatory RNAs, and mRNAs in live bacterial cells** *eLife* **10**:e64207 https://doi.org/10.7554/eLife.64207 | Google Scholar

71 Hamouche L., Poljak L., Carpousis A. J (2021) **Polyribosome-dependent clustering of membrane-anchored RNA degradosomes to form sites of mRNA degradation in Escherichia coli** *mBio* **12**:e1932–1921 https://doi.org/10.1128/mbio.01932-21 | Google Scholar

72 Hamouche L., et al. (2020) **Dynamic membrane localization of RNase Y in Bacillus subtilis** *mBio* **11**:e3337–3319 https://doi.org/10.1128/mbio.03337-19 | Google Scholar

73 Knight J. D., Lerner M. G., Marcano-Velázquez J. G., Pastor R. W., Falke Joseph J (2010) **Single molecule diffusion of membrane-bound proteins: window into lipid contacts and bilayer dynamics** *Biophysical Journal* **99**:2879–2887 https://doi.org/10.1016/j.bpj.2010.08.046 | Google Scholar

Author information

Laura Troyer*
Department of Physics, University of Illinois Urbana-Champaign, Urbana, United States
ORCID iD: 0000-0002-7208-6654

*These authors contributed equally.

Yu-Huan Wang*
Department of Physics, University of Illinois Urbana-Champaign, Urbana, United States
ORCID iD: 0009-0000-3086-1336

*These authors contributed equally.

Shobhna Shobhna
Theoretical and Computational Biophysics Group, NIH Center for Macromolecular Modeling and Visualization, Beckman Institute for Advanced Science and Technology, University of Illinois Urbana-Champaign, Urbana, United States, Department of Biochemistry, University of Illinois Urbana-Champaign, Urbana, United States
ORCID iD: 0009-0003-6831-2799

Seunghyeon Kim
Department of Physics, University of Illinois Urbana-Champaign, Urbana, United States
ORCID iD: 0009-0000-5450-8860

Brooke Ramsey
Center for Biophysics and Quantitative Biology, University of Illinois Urbana–Champaign, Urbana, United States

Jeechul Woo
Moduli Technologies, LLC, Springfield, United States

Emad Tajkhorshid
Theoretical and Computational Biophysics Group, NIH Center for Macromolecular Modeling and Visualization, Beckman Institute for Advanced Science and Technology, University of Illinois Urbana-Champaign, Urbana, United States, Department of Biochemistry, University of Illinois Urbana-Champaign, Urbana, United States, Center for Biophysics and Quantitative Biology, University of Illinois Urbana–Champaign, Urbana, United States
ORCID iD: 0000-0001-8434-1010

For correspondence: emad@illinois.edu

Sangjin Kim
Department of Physics, University of Illinois Urbana-Champaign, Urbana, United States, Center for Biophysics and Quantitative Biology, University of Illinois Urbana–Champaign, Urbana, United States
ORCID iD: 0000-0002-8444-7891

For correspondence: sangjin@illinois.edu

Editors

Reviewing Editor
Jie Xiao
Johns Hopkins University, Baltimore, United States of America

Senior Editor
Felix Campelo
Universitat Pompeu Fabra, Barcelona, Spain

Reviewer #1 (Public review):

This paper by Troyer et al. measures the positioning and diffusivity of RNaseE-mEos3.2 proteins in E. coli as a function of rifampicin treatment, compares RNaseE to other E. coli proteins, and measures the effect of changes in domain composition on this localization and motion. The straightforward study is thoroughly presented, including very good descriptions of the imaging parameters and the image analysis/modeling involved, which is good because the key impact of the work lies in presenting this clear methodology for determining the position and mobility of a series of proteins in living bacteria cells.

Most of my concerns in the original review were addressed in this round of revisions based on new text, experiments, and analysis, including most notably:

-A revision of the abstract to focus on the actual topic of the manuscript.
-New experiments (Fig. S1) to confirm that there is no significant undercounting of the fast-moving cytoplasmic population
-Removing the experiments discussion related to degradosome proteins rather than overstating results.
-Improving the logical flow and writing.

One minor concern still remains:

-Though the discussion of the rifampicin-treated cells is improved, this experiment is motivated (line 196) as "To test the effect of mRNA substrates on RNE diffusion", but the conclusion of the paragraph (based on similarities with the effect on LacY) is that the observed changes are due to factors other than the concentration of mRNA substrates, such that the effect of mRNA has not been tested.

https://doi.org/10.7554/eLife.105062.2.sa3

Reviewer #2 (Public review):

Summary:

Troyer and colleagues have studied the in vivo localisation and mobility of the E.coli RNaseE (a protein key for mRNA degradation in all bacteria) as well as the impact of two key protein segments (MTS and CTD) on RNase E cellular localisation and mobility. Such sequences are important to study since there is significant sequence diversity within bacteria, as well as lack of clarity about their functional effects. Using single-molecule tracking in living bacteria, the authors confirmed that >90% of RNaseE localised on the membrane, and measured its diffusion coefficient. Via a series of mutants, they also showed that MTS leads to stronger membrane association and slower diffusion compared to a transmembrane motif (despite the latter being more embedded in the membrane), and that the CTD weakens membrane binding. The study also rationalised how the interplay of MTS and CTD modulate mRNA metabolism (and hence gene expression) in different cellular contexts.

The authors have also done an excellent job addressing reviewer's concerns and improving the manuscript during revision.

https://doi.org/10.7554/eLife.105062.2.sa2

Reviewer #3 (Public review):

Summary:

The manuscript by Troyer et al quantitatively measured the membrane localization and diffusion of RNase E, an essential ribonuclease for mRNA turnover as well as tRNA and rRNA processing in bacteria cells. Using single-molecule tracking in live E. coli cells, the authors investigated the impact of membrane targeting sequence (MTS) and the C-terminal domain (CTD) on the membrane localization and diffusion of RNase E under various perturbations. Finally, the authors tried to correlate the membrane localization of RNase E to its function on co- and post-transcriptional mRNA decay using lacZ mRNA as a model.

The major findings of the manuscripts include:

(1) WT RNase E is mostly membrane localized via MTS, confirming previous results. The diffusion of RNase E is increased upon removal of MTS or CTD, and more significantly increased upon removal of both regions.

(2) By tagging RNase E MTS and different lengths of LacY transmembrane domain (LacY2, LacY6 or LacY12) to mEos3.2, the results demonstrate that short LacY transmembrane sequence (LacY2 and LacY6) can increase the diffusion of mEos3.2 on the membrane compared to MTS, further supported by the molecular dynamics simulation. The similar trend was roughly observed in RNase E mutants with MTS switched to LacY transmembrane domains.

(3) The removal of RNase E MTS significantly increases the co-transcriptional degradation of lacZ mRNA, but has minimal effect on the post-transcriptional degradation of lacZ mRNA. Removal of CTD of RNase E overall decrease the mRNA decay rates, suggesting the synergistic effect of CTD on RNase E activity.

Strengths:

(1) The manuscript is clearly written with very detailed methods description and analysis parameters.

(2) The conclusions are mostly supported by the data and analysis.

(3) Some of the main conclusions are interesting and important for understanding the cellular behavior and function of RNase E.

Weaknesses:

The authors have addressed my previous concerns in the revised manuscript.

Comments on revisions:

I have one additional comment. When interpreting the small increase in the diffusion coefficient of RNase E when treating the cell with rifampicin, the authors rule out the possibility that only a small fraction of RNase E interacts with mRNA and suggest that it is more likely the mRNA-RNase E interaction is transient. However, I am wondering about an alternative possibility that RNase E prefers mRNAs with low ribosome density or even untranslated mRNAs?

https://doi.org/10.7554/eLife.105062.2.sa1

Author response:

The following is the authors' response to the original reviews.

> ***Reviewer #1 (Public review):***
>
> *This paper measures the positioning and diffusivity of RNaseE-mEos3.2 proteins in E. coli as a function of rifampicin treatment, compares RNaseE to other E. coli proteins, and measures the effect of changes in domain composition on this localization and motion. The straightforward study is thoroughly presented, including very good descriptions of the imaging parameters and the image analysis/modeling involved, which is good because the key impact of the work lies in presenting this clear methodology for determining the position and mobility of a series of proteins in living bacteria cells.*

Thank you for the nice summary and positive feedback on the descriptions and methodology.

> *My key notes and concerns are listed below; the most important concerns are indicated with asterisks.*
>
> *(1) The very start of the abstract mentions that the domain composition of RNase E varies among species, which leads the reader to believe that the modifications made to E. coli RNase E would be to swap in the domains from other species, but the experiment is actually to swap in domains from other E. coli proteins. The impact of this work would be increased by examining, for instance, RNase E domains from B. subtilis and C. crescentus as mentioned in the introduction.*

Thank you for the suggestions. We agree that the sentence may convey an unintended expectation. Our original intention was to note the presence and absence of certain domains of RNase E (e.g. membrane-binding motif and CTD) vary across species, rather than the actual sequence variations. To avoid any misinterpretation, we decided to remove the sentence from the abstract. Using the domains of B. subtilis and C. crescentus RNase E in E. coli is a very interesting suggestion, but we will leave that for a future study.

> *(2) Furthermore, the introduction ends by suggesting that this work will modulate the localization, diffusion, and activity of RNase E for "various applications", but no applications are discussed in the discussion or conclusion. The impact of this work would be increased by actually indicating potential reasons why one would want to modulate the activity of RNase E.*

Thank you for this suggestion. For example, an E. coli strain expressing membranebound RNase E without CTD can help stabilize mRNAs and enhance protein expression. In fact, this idea was used in a commercial BL21 cell line (Invitrogen's One Shot BL21 Star), to increase the yield of protein expression. We also think that environmentally modulated MB% of RNase E can be useful for controlling the mRNA half-lives and protein expression levels in different conditions. We discussed these ideas at the end of the Discussion.

> *(3) Lines 114 - 115: "The xNorm histogram of RNase E shows two peaks corresponding to each side edge of the membrane": "side edge" is not a helpful term. I suggest instead: "...corresponding to the membrane at each side of the cell"*

Thank you. We made the suggested change.

> *(4) A key concern of this reviewer is that, since membrane-bound proteins diffuse more slowly than cytoplasmic proteins, some significant undercounting of the % of cytoplasmic proteins is expected due to decreased detectability of the faster-moving proteins. This would not be a problem for the LacZ imaging where essentially all proteins are cytoplasmic, but would significantly affect the reported MB% for the intermediate protein constructs. How is this undercounting considered and taken into account? One could, for*

> *instance, compare LacZ vs. LacY (or RNase E) copy numbers detected in fixed cells to those detected in living cells to estimate it.*

Thank you for raising this point and suggesting a possible way to address this. We compared the number of tracks for mEos3.2-fused proteins in live vs fixed cells and tested the undercounting effect of cytoplasmic molecules. We compared WT RNase E molecules in live and fixed cells and found that there are about 50% lower molecules detected in the fixed cells, which agrees with the expectation that fluorescent proteins lose their signal upon fixation. Similarly, cytoplasmic RNase E (RNase E ΔMTS) copy number was also ~50% less in the fixed cells compared to live cells. If cytoplasmic molecules were undercounted compared membrane-bound molecules in live cells, fixation would reduce the copy number less than 50%. The comparable ratio of 50% indicates that the undercounting issue is not significant. This control analysis is provided in Figure S1B-C, and we made corresponding textual change in the result section as below:

For this analysis, we first confirmed that proteins localized on the membrane and in the cytoplasm are detected with equal probability, despite differences in their mobilities (Fig. S1B-C).

> *(5) The rifampicin treatment study is not presented well. Firstly, it is found that LacY diffuses more rapidly upon rifampicin treatment. This change is attributed to changes in crowding at the membrane due to mRNA. Several other things change in cells after adding rif, including ATP levels, and these factors should be considered. More importantly, since the change in the diffusivity of RNaseE is similar to the change in diffusivity of LacY, then it seems that most of the change in RNaseE diffusion is NOT due to RNaseE-mRNAribosome binding, but rather due to whatever crowding/viscosity effects are experienced by LacY (along these lines: the error reported for D is SEM, but really should be a confidence interval, as in Figure 1, to give the reader a better sense of how different (or similar) 1.47 and 1.25 are).*

We agree with the reviewer that upon rifampicin treatment, RNase E's D increases to a similar extent as that of LacY. Hence, the increase likely arises from a factor common to both proteins. We have added the reviewer's suggested interpretation as a possible explanation in the manuscript as below.

The similar fold change in D_{RNE} and D_{LacY} upon rif treatment suggests that the change in RNE diffusion may largely be attributed to physical changes in the intracellular environment (such as reduced viscosity or macromolecular crowding[41,42]), rather than a loss of RNA-RNE interactions.

As requested by the reviewer, we have provided confidence intervals for our D values in Table S8. Because these intervals are very narrow, we chose to present the SEM as the error metric for D and have also reported the corresponding errors for the fold-change values whenever we describe the fold differences between D values.

> *(6) Lines 185-189: it is surprising to me that the CTD mutants both have the same change in D (5.5x and 5.3x) relative to their full-length counterparts since D for the membranebound WT protein should be much less sensitive to protein size than D for the cytoplasmic MTS mutant. Can the authors comment?*

Perhaps the reviewer understood that these differences are the ratios between +/-CTD (e.g. WT RNE vs ΔCTD). However, the differences we mentioned were from membrane-bound vs cytoplasmic versions of RNase E with comparable sizes (e.g. WT RNase E vs RNase E ΔMTS). We modified text and added a summary sentence at the end of the paragraph to clarify the point.

We found that $D_{\Delta MTS}$ is ~5.5 times that of D_{RNE} (Fig. 3B). [...] Together, these results suggest that the membrane binding reduces RNE mobility by a factor of 5.

That being said, we also realized a similar fold difference between +/-CTD. Specifically, WT RNE vs RNE ΔCTD (both membrane-bound) show a ~4.1-fold difference and RNE ΔMTS vs RNE ΔMTS ΔCTD (both cytoplasmic) show ~3.9-fold difference. We do not currently do not have a clear explanation for this pattern. Given that these two pairs have a similar change in mass, we speculate that the relationship between D and molecular mass may be comparable for membrane-bound and free-floating RNE variants.

> *(7) Lines 190-194. Again, the confidence intervals and experimental uncertainties should be considered before drawing biological conclusions. It would seem that there is "no significant change" in the rhlB and pnp mutants, and I would avoid saying "especially for Δpnp" when the same conclusion is true for both (one shouldn't say 1.04 is "very minute" and 1.08 is just kind of small - they are pretty much the same within experiments like this).*

Thank you for raising this point, which we fully agree with. That being said, we decided to remove results related to the degradosome proteins to improve the flow of the paper. We are preparing another paper related to the RNA degradosome complex formation.

> *(8) Lines 221-223 " This is remarkable because their molecular masses (and thus size) are expected to be larger than that of MTS" should be reconsidered: diffusion in a membrane does not follow the Einstein law (indeed lines 223-225 agree with me and disagree with lines 221-223). (Also the discussion paragraph starting at line 375). Rather, it is generally limited by the interactions with the transmembrane segments with the membrane. So Figure 3D does not contain the right data for a comparison, and what is surprising to me is that MTS doesn't diffuse considerably faster than LacY2.*

We agree with the reviewer's point that diffusion in a membrane does not follow the Stokes-Einstein law. That is why we introduced Saffman's model. However, even in this model, proteins of larger size (or mass) should be slower than smaller size (a reason why we presented Figure 3D, now 4D). In other words, both Einstein and Saffman models predict that larger particles diffuse slower, although the exact scaling relationship differs between two models. Here, we assume that mass is related to the size. Contrary to Saffman's model for membrane proteins, LacY2 diffuses faster than MTS despite of large size. Using MD simulations, we showed that this discrepancy can be explained by different interaction energies as the reviewer mentioned. This analysis further demonstrates that the size is not the only factor to consider protein diffusion in the membrane. We edited the paragraph to clarify the expectations and our interpretations.

According to the Stokes-Einstein relation for diffusion in simple fluids[49] and the Saffman-Delbruck diffusion model for membrane proteins, D decreases as particle size increases, albeit with different scaling behaviors. [...] Thus, if size (or mass) were the primary determinant of diffusion, LacY2 and LacY6 would diffuse more slowly than the smaller MTS. The observed discrepancy instead implies that D may be governed by how each motif interacts with the membrane. For example, the way that TM domains are anchored to the membrane may facilitate faster lateral diffusion with surrounding lipids.

> *(9) The logical connection between the membrane-association discussion (which seems to ignore associations with other proteins in the cell) and the preceding +/- rifampicin discussion (which seeks to attribute very small changes to mRNA association) is confusing.*

Thank you for raising this point. We re-arranged the second result section to present diffusion due to membrane binding first before rifampicin. Furthermore, we stated our hypothesis and expectations in the beginning of the results section. This addition will legitimate our logic flow.

> *(10) Separately, the manuscript should be read through again for grammar and usage. For instance, the title should be: "Single-molecule imaging reveals the *roles* of *the* membrane-binding motif and *the* C-terminal domain of RNase E in its localization and diffusion in Escherichia coli". Also, some writing is unwieldy, for instance, "RNase E's D" would be easier to read if written as D_{RNaseE}. (underscore = subscript), and there is a lot of repetition in the sentence structures.*

Thank you for catching grammar mistakes. We went through extensive proofreading to avoid these mistakes and also used simple notation suggested by the reviewer, such as D_{RNE}, to make it easier to read. Thank you again for your suggestions.

> ***Reviewer #2 (Public review):***
>
> *Summary:*
>
> *Troyer and colleagues have studied the in vivo localisation and mobility of the E.coli RNaseE (a protein key for mRNA degradation in all bacteria) as well as the impact of two key protein segments (MTS and CTD) on RNase E cellular localisation and mobility. Such sequences are important to study since there is significant sequence diversity within bacteria, as well as a lack of clarity about their functional effects. Using single-molecule tracking in living bacteria, the authors confirmed that >90% of RNaseE localised on the membrane, and measured its diffusion coefficient. Via a series of mutants, they also showed that MTS leads to stronger membrane association and slower diffusion compared to a transmembrane motif (despite the latter being more embedded in the membrane), and that the CTD weakens membrane binding. The study also rationalised how the interplay of MTS and CTD modulate mRNA metabolism (and hence gene expression) in different cellular contexts.*
>
> *Strengths:*
>
> *The study uses powerful single-molecule tracking in living cells along with solid quantitative analysis, and provides direct measurements for the mobility and localisation of E.coli RNaseE, adding to information from complementary studies and other bacteria. The exploration of different membrane-binding motifs (both MTS and CTD) has novelty and provides insight on how sequence and membrane interactions can control function of protein-associated membranes and complexes. The methods and membrane-protein standards used contribute to the toolbox for molecular analysis in live bacteria.*

Thank you for the nice summary of our work and positive comments about the paper's strengths.

> *Weaknesses:*
>
> *The Results sections can be structured better to present the main hypotheses to be tested. For example, since it is well known that RNase E is membrane-localised (via its MTS), one expects its mobility to be mainly controlled by the interaction with the membrane (rather than with other molecules, such as polysomes and the degradosome). The results indeed support this expectation - however, the manuscript in its current form does not lay down the dominant hypothesis early on (see second Results chapter), and instead considers the*

> *rifampicin-addition results as "surprising"; it will be best to outline the most likely hypotheses, and then discuss the results in that light.*

Thank you for this comment. We addressed this point by stating our main hypothesis from the beginning of the results section. We also agree with the reviewer that the membrane binding effect should be discussed first; hence, we re-arranged the result section. In the revised manuscript, we discuss the effect of membrane binding on diffusion first, followed by rif effects.

> *Similarly, the authors should first discuss the different modes of interaction for a peripheral anchor vs a transmembrane anchor, outline the state of knowledge and possibilities, and then discuss their result; in its current version, the ms considers the LacY2 and LacY6 faster diffusion compared to MTS "remarkable", but considering the very different mode of interaction, there is no clear expectation prior to the experiment. In the same section, it would be good to see how the MD simulations capture the motion of LacY6 and LacY12, since this will provide a set of results consistent with the experimental set.*

Thank you for pointing this out. In fact, there is little discussion in the literature about the different modes of interaction for a peripheral anchor vs a transmembrane anchor. To our knowledge, our work (experiments and MD simulations) is the first that directly compared the two to reveal that the peripheral anchor has higher interaction energy than the transmembrane anchor. We added a sentence “Despite the prevalence of peripheral membrane proteins, how they interact with the membrane and how this differs from TM proteins remain poorly understood”. Furthermore, we added the MD simulation result of LacY6 and LacY12 in Figure 4E-F.

> *The work will benefit from further exploration of the membrane-RNase E interactions; e.g., the effect of membrane composition is explored by just using two different growth media (which on its own is not a well-controlled setting), and no attempts to change the MTS itself were made. The manuscript will benefit from considering experiments that explore the diversity of RNaseE interactions in different species; for example, the authors may want to consider the possibility of using the membrane-localisation signals of functional homologs of RNaseE in different bacteria (e.g., B. subtilis). It would be good to look at the effect of CTD deletions in a similar context (i.e., in addition to the MTS substitution by LacY2 and LacY6).*

Thank you very much for this suggestion. During revision, we engineered point mutations in MTS and analyzed critical hydrophobic residues for membrane binding. We characterized MB% in both +/-CTD variants (Fig. 2 and Fig. S6) and their effect on lacZ mRNA degradation (Fig. 6). We will leave the use of membrane motif of B. subtilis RNase E for future study.

> *The manuscript will benefit from further discussion of the unstructured nature of the CTD, especially since the RNase CTD is well known to form condensates in Caulobacter crescentus; it is unclear how the authors excluded any roles for RNaseE phase separation in the mobility of RNaseE in E.coli cells.*

Yes, we agree with the reviewer that the intrinsically disordered nature of the CTD might contribute to condensate formation. We explored this possibility using both epifluorescence microscopy (with a YFP fusion) and single-molecule imaging with cluster analysis (using an mEos3.2 fusion). Please see Figure S8. We did observe some weak de-clustering of RNase E upon CTD deletion. In the current study, we are unable to quantify the extent to which clustering contributes to the slow diffusion of RNase E. However, we speculate that the

clustering may be linked to the low MB% of certain RNE mutants containing CTD, and we discussed this possibility in the Discussion.

[…] further supporting that the CTD decreases membrane association across RNE variants. We speculate that this effect may be related to the CTD's role in promoting phase-separated ribonucleoprotein condensates, as observed in Caulobacter crescentus[19]. In E. coli, we also observed a modest increase in the clustering tendency of RNE compared to ΔCTD (Fig. S8).

> *Some statements in the Discussion require support with example calculations or toning down substantially. Specifically, it is not clear how the authors conclude that RNaseE interacts with its substrate for a short time (and what this time may actually be); further, the speculation about the MTS "not being an efficient membrane-binding motif for diffusion" lacks adequate support as it stands.*

Thank you for these points. To elaborate our point on transient interaction between RNase E and RNA, we added a sentence "Specifically, if RNE interacts with mRNAs for ~20 ms or less, the slow-diffusing state would last shorter than the frame interval and remain undetected in our experiment." Also, we added this sentence in the discussion.

One possible explanation is that RNA-bound RNE (and RNase Y) is short-lived compared to our frame interval (~20 ms), unlike other RNA-binding proteins related to transcription and translation, interacting with RNA for ~1 min for elongation [48].

Plus, we clarified the wording used in the second sentence that the reviewer pointed out as follows,

Lastly, the slow diffusion of the MTS in comparison to LacY2 and LacY6 suggests that MTS is less favorable for rapid lateral motion in the membrane.

> ***Reviewer #3 (Public review):***
>
> *Summary:*
>
> *The manuscript by Troyer et al quantitatively measured the membrane localization and diffusion of RNase E, an essential ribonuclease for mRNA turnover as well as tRNA and rRNA processing in bacteria cells. Using single-molecule tracking in live E. coli cells, the authors investigated the impact of membrane targeting sequence (MTS) and the Cterminal domain (CTD) on the membrane localization and diffusion of RNase E under various perturbations. Finally, the authors tried to correlate the membrane localization of RNase E to its function on co- and post-transcriptional mRNA decay using lacZ mRNA as a model.*
>
> *The major findings of the manuscripts include:*
>
> *(1) WT RNase E is mostly membrane localized via MTS, confirming previous results. The diffusion of RNase E is increased upon removal of MTS or CTD, and more significantly increased upon removal of both regions.*
>
> *(2) By tagging RNase E MTS and different lengths of LacY transmembrane domain (LacY2, LacY6, or LacY12) to mEos3.2, the results demonstrate that short LacY transmembrane sequence (LacY2 and LacY6) can increase the diffusion of mEos3.2 on the membrane compared to MTS, further supported by the molecular dynamics simulation. A similar trend was roughly observed in RNase E mutants with MTS switched to LacY transmembrane domains.*
>
> *(3) The removal of RNase E MTS significantly increases the co-transcriptional degradation of lacZ mRNA, but has minimal effect on the post-transcriptional degradation of lacZ*

> *mRNA. Removal of CTD of RNase E overall decreases the mRNA decay rates, suggesting the synergistic effect of CTD on RNase E activity.*
>
> *Strengths:*
>
> *(1) The manuscript is clearly written with very detailed method descriptions and analysis parameters.*
>
> *(2) The conclusions are mostly supported by the data and analysis.*
>
> *(3) Some of the main conclusions are interesting and important for understanding the cellular behavior and function of RNase E.*

Thank you for your thorough summary of our work and positive comments.

> *Weaknesses:*
>
> *(1) Some of the observations show inconsistent or context-dependent trends that make it hard to generalize certain conclusions. Those points are worth discussion at least. Examples include:*
>
> *(a) The authors conclude that MTS segment exhibits reduced MB% when succinate is used as a carbon source compared to glycerol, whereas LacY2 segment maintains 100% membrane localization, suggesting that MTS can lose membrane affinity in the former growth condition (Ln 341-342). However, the opposite case was observed for the WT RNase E and RNase E-LacY2-CTD, in which RNase E-LacY2-CTD showed reduced MB% in the succinate-containing M9 media compared to the WT RNase E (Ln 264-267). This opposite trend was not discussed. In the absence of CTD, would the media-dependent membrane localization be similar to the membrane localization sequence or to the fulllength RNase E?*

This is a great point. Thank you for pointing out the discrepancy in data. We think the weak membrane interaction of RNaseE-lacY2-CTD likely stems from the structure instability in the presence of the CTD. Our data shows that an RNase E variant with a cytoplasmic population under a normal growth condition exhibits a greater cytoplasmic fraction in a poor growth media. In contrast, RNaseE-MTS and RNaseE-LacY2 lacking the CTD both showed 100% MB% under both normal and poor growth conditions. These results are presented in Figure S6 and further discussed in the Discussion section.

The loss of MB% in LacY2-based RNE was observed only in the presence of the CTD (Fig. S6D), suggesting that the CTD negatively affects membrane binding of RNE, possibly by altering protein conformation. In fact, all ΔCTD RNE mutants we tested exhibited higher MB% than their CTD-containing counterparts (Fig. S6A-B).

> *(b) When using mEos3.2 reporter only, LacY2 and LacY6 both increase the diffusion of mEos3.2 compared to MTS. However, when inserting the LacY transmembrane sequence into RNase E or RNase E without CTD, only the LacY2 increases the diffusion of RNase E. This should also be discussed.*

Thank you for raising this point. As the reviewer pointed out, as the membrane motifs, both LacY2 and LacY6 diffuse faster than the MTS, but when they are fused to RNE, only LacY2-based RNE diffuses faster than MTS-based RNE. We speculate that it is possibly due to a structural reason—having four (large) LacY6 in a tetrameric arrangement may cancel out the original fast-diffusing property of LacY6. We added this idea in the result section:

This result may be due to the high TM load (24 helices) created by four LacY6 anchors in the RNE tetramer. Although all constructs are tetrameric, the 24-helix load (LacY6), compared

with 8 (LacY2) and 4 (MTS), likely enlarges the membrane-embedded footprint and increases drag, thereby changing the mobility advantages assessed as standalone membrane anchors.

> *(2) The authors interpret that in some cases the increase in the diffusion coefficient is related to the increase in the cytoplasm localization portion, such as for the LacY2 inserted RNase E with CTD, which is rational. However, the authors can directly measure the diffusion coefficient of the membrane and cytoplasm portion of RNase E by classifying the trajectories based on their localizations first, rather than just the ensemble calculation.*

Thank you for this suggestion. Currently, because of the 2D projection effect from imaging, we cannot clearly distinguish which individual tracks are from the cytoplasm or from the inner membrane based on the localization. Therefore, we are unable to assign individual tracks as membrane-bound or cytoplasmic. However, we can demonstrate that the xNorm data can be separated into two different spatial populations based on the diffusion coefficient. D. That is we can plot xNorm of slow tracks vs xNorm of fast tracks. This analysis showed that the slow tracks have LacY-like xNorm profiles while the fast tracks have LacZ-like xNorm profiles, also quantitatively supporting our MB% fitting results. We have added this analysis to Figure S2.

> *(3) The error bars of the diffusion coefficient and MB% are all SEM from bootstrapping, which are very small. I am wondering how much of the difference is simply due to a batch effect. Were the data mixed from multiple biological replicates? The number of biological replicates should also be reported.*

Thank you for raising this point. In the original manuscript, we reported the number of tracks analyzed and noted that all data was from at least three separate biological replicates (measurements were repeated at least three different days). Furthermore, in the revised manuscript, we have provided the number of cells imaged in Table S6.

> *(4) Some figures lack p-values, such as Figures 4 and 5C-D. Also, adding p-values directly to the bar graphs will make it easier to read.*

Thank you for checking these details. We added p values in the graphs showing k_{d1} and k_{d2} (Table S7).

> ***Reviewer #2 (Recommendations for the authors):***
>
> *Minor and technical points:*
>
> *(1) Clarity and flow will be improved if each section first highlights the objective for the experiments that are described (e.g., line 240).*

Thank you for the suggestion. We addressed this point by editing the beginning of each subsection in the Results.

> *(2) Line 272 (and elsewhere)."1.33-times faster is wrong". The authors mean 33% faster (from 0.075 to 1, see Figure 4G), and not 133% faster. Needs fixing.*

Thanks for pointing this out. We changed this as well as other incidences where we talk about the fold difference. For example, this particular incidence was changed to:

Indeed, in the absence of the CTD, we found that the D of LacY2-based RNE was 1.33 ± 0.01 times as fast as the MTS-based RNE.

> *(3) The authors need to consider the fitting of two species on their D population. e.g., how will a 93% - 7% split between diffusive species would have looked for the distribution in S4B? Note also the L1 profile in Fig S4C - while it is not hugely different from Figure S4B, the analysis gives a 41% amplitude for the fast-diffusing species. The 2-species analysis can also be used on some of the samples with much higher cytoplasmic components. Further, tracks that are in the more central region can be analysed to see whether the fast-diffusing species increase in amplitude.*

Thank you for this comment. The D histograms of L1 and RNase E show a dominant peak at around 0.015, but L1 has a residual population in the shoulder (note the difference between L1's experimental data and D1 fit, a yellow line in now Figure S3B). This residual shoulder population is absent in the D histogram of RNase E. We also performed two-species analysis as suggested by the reviewer and provided the result in Figure S3C. The analysis shows that the two-population fit (black line) is very close to one one-population fit (yellow line). While we agree with the reviewer that subpopulation analysis is helpful for other proteins that show <90% MB% (>10% significant cytoplasmic population). we found it useful to divide xNorm histogram into two populations based on the diffusivity (rather than doing two-population fit to the D histogram, which does not have spatial information). This analysis, shown in Figure S2, supports our MB% fit results.

> *(4) The authors suggest that the sequestration of RNaseE to the membrane limits its interaction with cytoplasmic mRNAs, and may increase mRNA lifetime. While this is true and supported by the authors' preprint (Ref15), it will also be good to consider (and discuss) that highly-transcribed regions are in the nucleoid periphery (and thus close to the membrane) and that ribosomes/polysomes are likewise predominantly peripheral (coregulation of transcription/translation) and membrane proximal.*

This is an interesting point, which we appreciate very much. The lacZ gene, when induced, is shown to move to the nucleoid periphery (Yang et al. 2019, Nat Comm). Also, in our preprint (Ref 15), we engineered to have lacZ closer to the membrane, by translationally fusing it to lacY. However, the degradation rate of lacZ mRNA was not enhanced by the proximity to the membrane (for both k_{d1} and k_{d2}). For lacZ mRNA, we mainly see the change in k_{d1} when RNE localization changes. We think it is due to the slow diffusion of the nascent mRNA (attached to the chromosome) and the slow diffusion of membrane-bound RNE, such that regardless of the location of the nascent mRNA, the degradation by the membrane-bound RNE is inefficient. Only when RNE is free diffusing in the cytoplasm, it seems to increase k_{d1} (the decay of nascent mRNAs).

> ***Reviewer #3 (Recommendations for the authors):***
>
> *(1) It will increase the clarity of the manuscript if the authors can provide better nomenclatures for different constructs, such as for different membrane targeting sequences fused to mEos3.2, full-length RNase E, or CDT truncated RNaseE.*

Thank you for this suggestion. We agree that many constructions were discussed, and their naming can be confusing. To help with clarity, we have abbreviated RNase E as RNE throughout the text where appropriate.

> *(2) Line 342, Figure S7D should be cited instead of S6D.*

Thank you for finding this error. We made a proper change in the revised manuscript.

https://doi.org/10.7554/eLife.105062.2.sa0